Title
Modeling and Control of HOT Lanes

Author
Horowitz, Roberto

Publication Date
2016-07-24

Modeling and Control of HOT Lanes

Roberto Horowitz, Alex A. Kurzhanskiy, Asfand Siddiqui, Mathew Wright

July 24, 2016

Contents

List of Figures

List of Tables

Acknowledgement

We would like to express great appreciation to our colleagues, former and current UC Berkeley researchers, Ajith Muralidharan for sharing ideas, Ramtin Pedarsani, Brian Phegley and Pravin Varaiya for their critical reading and their help in clarifying some theoretical issues.

This research was sponsored by the Division of Research, Innovation and System Information (DRISI) of the California Department of Transportation.

Chapter 1

Introduction

1.1 Overview

This report describes the *macroscopic* simulation model of freeways with High-Occupancy Vehicle (HOV) and High-Occupancy or Tolled (HOT) lanes, and its calibration methodology. It is organized as follows.

- Chapter 2 covers the project methodology.
  - Section 2.1 introduces the underlying traffic model.
  - Section 2.2 shows how the proposed traffic model accommodates different HOV lane configurations.
  - Section 2.3 explains how this model is extended to incorporate an HOT lane.
  - Section 2.5 discusses model calibration issues.
  - Section 2.4 addresses the calibration of the HOT controller.

Data analysis and simulation results are presented in Chapters 3-5.

- Chapter 3 presents the model of I-680 North freeway in Contra Costa County with full access HOV lane.

- Chapter 4 presents the model of I-210 East freeway in Los Angeles County with limited access HOV lane.
- Chapter 5 presents the model of the HOT controller calibrated based on the FasTrak transponder data on I-10 West in Los Angeles County.
- Chapter 6 concludes the report.

1.2 Problem

The Texas A&M Transportation Institute (TTI) Urban Mobility Report [11] finds that congestion forced urban Americans to travel 5.5 billion hours more and waste 2.9 billion gallons of fuel at a cost of $121 billion in 2011. Inefficient traffic management, and/or demand that exceeds road network capacity are the most common causes of recurrent congestion. One way to reduce demand is to encourage carpools through an HOV lane. With fewer vehicles, a trip in the HOV lane will take less time than a trip in the general purpose (GP) lane. Intended to reward people that travel in groups by providing a shorter travel time, HOV lanes were criticized for being underutilized, thereby worsening the overall traffic congestion on freeways. This criticism led to the concept of HOT lanes. Available to high-occupancy vehicles without charge, HOT lane admits other vehicles if they pay a fee.[1] Acceptance of more than just high-occupancy vehicles should lead to higher utilization of HOT lanes compared to their HOV counterparts. However, as was pointed out in [10], currently some HOT implementations do not deliver what their planners promised. According to traffic measurements, HOT lanes either provide no advantage in terms of travel time over the GP lanes, or, being heavily underutilized, degrade the performance of the whole freeway congesting GP lanes more than necessary. Thus, proper operation of HOV/T lanes requires the combination of both, effective supply and demand management. There is a need for methods and tools that enable quick quantitative assessment of scenarios and operational strategies in terms of benefits they provide for freeways with HOV/T lanes.

The research described in the current report builds upon the work conducted in 2006-14 in the

[1] The fee may be fixed or adjustable based on the demand.

Caltrans-sponsored UC Berkeley projects, Tools for Operational Planning (TOPL) [16] and Connected Corridors [2]. Our proposed HOV/T model is a modification of the Link-Node Cell Transmission Model [9] developed by TOPL. To validate our model, we used Berkeley Advanced Traffic Simulator (BeATS) [1] developed by Connected Corridors.

1.3 Objective

The aim of the current project was to develop a macroscopic freeway simulation model with an HOV/T lane, which could be calibrated based on measured vehicle counts and speeds and used for efficient evaluation of operational scenarios on freeways with HOV/T lanes.

Working toward this goal, we delivered:

1. Theoretical model of a freeway with an HOV/T lane;
2. HOT lane control algorithm;
3. Implementation of the HOV/T model and the HOT control algorithm in BeATS;
4. Calibration methodology for the proposed model; and
5. Evaluation of proposed algorithms using I-680 North and I-210 East freeway data.

1.4 Scope

Current list of HOT lane facilities in California is given in Table 1.1, spanning over 180 miles. HOT facilities are becoming popular in the U.S. For example, in the San Francisco Bay Area alone, the Metropolitan Transportation Commission (MTC) promises the implementation of a 550-mile express lane network by 2035, and all of it will be managed with dynamic pricing strategies.

Facility	Description
I-10	14 miles in each direction
I-15	20 miles in each direction
I-110	11 miles in each direction
I-580	14 miles in each direction
I-680 Milpitas - Sunol	14 miles South Bound
I-880 / SR-237	4 miles in each direction
SR-91	10 miles in each direction
I-680 San Ramon - Walnut Creek	12 miles in each direction expected to open in spring 2017

Table 1.1: List of HOT facilities in California.

Proper deployment and management of HOV/T facilities relies on the continuous process of:

1. obtaining and analyzing traffic measurement data;
2. operations planning — simulating various scenarios and operational strategies; and
3. implementing the most promising operational strategies in the field.

This process requires a fast and trusted traffic simulator for the rapid quantitative assessment of a large number of operational strategies for the road network under various scenarios. The research presented hereby is the stepping stone for achieving this goal.

Chapter 2

Methodology

2.1 Traffic Model

We model traffic flow in a road network consisting of links $\mathcal{L}$ and nodes $\mathcal{N}$, where links represent stretches of roads, and nodes represent junctions that connect links. A node always has at least one input and at least one output link. A link is called *ordinary* if it has both begin and end nodes. A link with no begin node is called *origin*, and a link with no end node is called *destination*. Origins are links through which vehicles enter the system, and destinations are links that let vehicles out. The traffic state at each moment of time is defined by the number of vehicles of different classes in every link. Different vehicle classes are needed to distinguish between low-occupancy vehicles (LOVs) and high-occupancy vehicles (HOVs). For HOT lanes the additional class is needed — LOVs ready to pay. The traffic model consists of three parts:

1. the node model that determines how flows entering a node are distributed between the node output links;
2. controllers that are responsible for traffic assignment, certain driver behavioral effects and flow control; and
3. the vehicle conservation law in links.

In this Section we start by discussing the node model, then address the local traffic assignment problem, and conclude by formally presenting the traffic model that we refer to as the Link-Node Cell Transmission Model (LNCTM).

2.1.1 Node Model

We shall use the node model that was presented in [17]. The notation for the node model is summarized below:

- M — number of input links.
- i — index of an input link ($i = 1, \ldots, M$).
- N — number of output links.
- j — index of an output link ($j = 1, \ldots, N$).
- C — number of commodities.
- c — index of a commodity ($c = 1, \ldots, C$).
- S_i^c — how much traffic of commodity c input i wants to send (demand or sending function), $S_i = \sum_{c=1}^{C} S_i^c$.
- p_i — input link priority.
- R_j — how much traffic output j can receive (supply or receive function).
- $\beta_{ij}^c \in [0, 1]$ — split ratios that distribute traffic of a given commodity c coming from input link i between output links, $\sum_{j=1}^{N} \beta_{ij}^c = 1$.
- $S_{ij}^c = \beta_{ij}^c S_i^c$ — oriented demand for commodity c from input link i to output link j, $S_{ij} = \sum_{c=1}^{C} S_{ij}^c$.
- $\boldsymbol{\eta}_{j'j}^i = [y, z] \subseteq [0, 1]$ — mutual restriction intervals that should be interpreted as follows:

- $\boldsymbol{\eta}_{j'j} = [0,1]$ — congestion in the output link j' affects flow directed from the input link i to the output link j in full. This is equivalent to the FIFO condition. Obviously, $\boldsymbol{\eta}^i_{jj} \equiv [0,1]$ for all i.
- $\boldsymbol{\eta}^i_{j'j} = [0,0]$ (or any other interval of zero length) — traffic state in the output link j' does not influence the flow from the input link i to the output link j. This is equivalent to no FIFO restriction.
- $\boldsymbol{\eta}^i_{j'j} = [y,z] \subset [0,1]$ — traffic state in the output link j' affects a $|\boldsymbol{\eta}^i_{j'j}| = z - y$ portion of the flow directed from the input link i to the output link j. We specify this influence as an interval, not just a scalar, to capture the summary effect of multiple output links that may restrict flow to the output link j.

- f^c_{ij} — input-output flows that the node model computes, $f_{ij} = \sum_{c=1}^{C} f^c_{ij}$.

Given the input demand per commodity, input link priorities, output supply and known split ratios, the following algorithm computes the flows going from input to output links at every node [17]:

1. Initialize:

$$\begin{aligned}
\tilde{R}_j(0) &:= R; \\
U_j(0) &:= U_j; \\
\tilde{S}^c_{ij}(0) &:= S^c_{ij}; \\
\tilde{S}_{ij}(0) &:= \sum_{c=1}^{C} \tilde{S}^c_{ij}(0); \\
\tilde{\boldsymbol{\eta}}^i_j(0) &:= [0,0]; \\
k &:= 0; \\
& \qquad i = 1,\ldots,M, \quad j = 1,\ldots,N, \quad c = 1,\ldots,C.
\end{aligned}$$

2. Define the set of output links that still need processing:

$$V(k) = \{j : \; U_j(k) \neq \emptyset\}\,.$$

If $V(k) = \emptyset$, stop.

3. Check that at least one of the unprocessed input links has nonzero priority, otherwise, assign equal positive priorities to all the unprocessed input links:

$$\tilde{p}_i(k) = \begin{cases} p_i, & \text{if there exists } i' \in \bigcup_{j \in V(k)} U_j(k) : \ p_{i'} > 0, \\ \frac{1}{\left|\bigcup_{j \in V(k)} U_j(k)\right|}, & \text{otherwise,} \end{cases} \tag{2.1.1}$$

where $\left|\bigcup_{j \in V(k)} U_j(k)\right|$ denotes the number of elements in the union $\bigcup_{j \in V(k)} U_j(k)$; and for each output link $j \in V(k)$ and input link $i \in U_j(k)$ compute oriented priority:

$$\tilde{p}_{ij}(k) = \tilde{p}_i(k) \frac{\sum_{c=1}^{C} S_{ij}^c}{\sum_{c=1}^{C} S_i^c}. \tag{2.1.2}$$

4. For each $j \in V(k)$, compute factors:

$$a_j(k) = \frac{\tilde{R}_j(k)}{\sum_{i \in U_j(k)} \tilde{p}_{ij}(k)}, \tag{2.1.3}$$

and find the smallest of these factors:

$$a_{j^*}(k) = \min_{j \in V(k)} a_j(k). \tag{2.1.4}$$

The link j^* has the most restricted supply of all output links.

5. Define the set of input links, whose demand does not exceed the allocated supply:

$$\tilde{U}(k) = \left\{ i \in U_{j^*}(k) : \ \left(\sum_{j \in V(k)} \tilde{S}_{ij}(k) \right) \leq \tilde{p}_i(k) a_{j^*}(k) \right\}.$$

- If $\tilde{U}(k) \neq \emptyset$, then for all output links $j \in V(k)$ assign:

$$\begin{aligned} f_{ij}^c &= \tilde{S}_{ij}^c(k), \quad i \in \tilde{U}(k), \ \ c = 1, \ldots, C; \\ \tilde{R}_j(k+1) &= \tilde{R}_j(k) - \sum_{i \in \tilde{U}(k)} f_{ij}; \\ U_j(k+1) &= U_j(k) \setminus \tilde{U}(k). \end{aligned} \tag{2.1.5}$$

- Else, for all input links $i \in U_{j^*}(k)$, output links $j \in V(k)$ and commodities $c = 1, \ldots, C$, assign:

$$\begin{aligned}
\tilde{S}^c_{ij^*}(k+1) &= \tilde{S}^c_{ij^*}(k)\frac{\tilde{p}_{ij^*}(k)a_{j^*}(k)}{\tilde{S}_{ij^*}(k)}, \quad c = 1, \ldots, C; && (2.1.6)\\
\tilde{S}^c_{ij}(k+1) &= \tilde{S}^c_{ij}(k)\frac{\tilde{S}_{ij}(k+1)}{\tilde{S}_{ij}(k)}, \;\; i \in U_j(k) \cap U_{j^*}(k), \;\; j \in V(k) \setminus \{j^*\}, && (2.1.7)
\end{aligned}$$

where

$$\begin{aligned}
\tilde{S}_{ij}(k+1) &= \tilde{S}_{ij}(k) - S_{ij}\left(|\boldsymbol{\eta}^i_{j^*j}| - |\tilde{\boldsymbol{\eta}}^i_j(k) \cap \boldsymbol{\eta}^i_{j^*j}|\right)\\
&\quad \times \left(1 - \frac{\sum_{c=1}^{C} \tilde{S}^c_{ij^*}(k+1)}{S_{ij^*}}\right); && (2.1.8)\\
\tilde{S}^c_{ij}(k+1) &= \tilde{S}^c_{ij}(k), \quad i \notin U_j(k) \cap U_{j^*}(k);\\
\tilde{\boldsymbol{\eta}}^i_j(k+1) &= \tilde{\boldsymbol{\eta}}^i_j(k) \cup \boldsymbol{\eta}^i_{j^*j};\\
f^c_{ij} &= \tilde{S}^c_{ij}(k+1), \quad i \in U_j(k) \cap U_{j^*}(k), \; j \in V(k) :\\
&\quad \tilde{\boldsymbol{\eta}}^i_j(k+1) = [0,1], \; c = 1, \ldots, C; && (2.1.9)\\
\tilde{R}_j(k+1) &= \tilde{R}_j(k) - \sum_{i \in U_{j^*}(k) : \boldsymbol{\eta}^i_j(k+1) = [0,1]} f_{ij};\\
U_j(k+1) &= U_j(k) \setminus \left\{ i \in U_{j^*}(k) : \; \tilde{\boldsymbol{\eta}}^i_j(k+1) = [0,1] \right\}.
\end{aligned}$$

6. Set $k := k + 1$, and return to step 2.

This algorithm takes no more than $(M + N - 2)$ iterations to complete. It is invoked on all nodes of the road network at each time step of the LNCTM.

2.1.2 Split Ratio Assignment

For a node with M input links, N output links and C commodities, where some of the split ratios β^c_{ij} are not defined a priori, they must be computed as functions of the input demand S^c_i, priorities p_i and the output supply R_j, $i = 1, \ldots, M$, $j = 1, \ldots, N$ and $c = 1, \ldots, C$. The algorithm for computing undefined split ratios is based on the following definitions and assumptions:

- Define the set of commodity movements, for which split ratios are known, $\mathcal{B} = \left\{ \{i, j, c\} : \; \beta^c_{ij} \in [0,1] \right\}$, and the set of commodity movements, for which split ratios are to be

computed, $\overline{\mathcal{B}} = \Big\{\{i,j,c\} :\ \beta_{ij}^c \text{ are unknown}\Big\}$.

- For a given input link i and commodity c such that $S_i^c = 0$, assume that all split ratios are known: $\{i,j,c\} \in \mathcal{B}$.[1]

- Define the set of output links, for which there exist unknown split ratios, $V = \big\{j :\ \exists\, \{i,j,c\} \in \overline{\mathcal{B}}\big\}$.

- Assuming that for a given input link i and commodity c split ratios must sum up to 1, define the unassigned portion of flow $\overline{\beta}_i^c = 1 - \sum_{j:\{i,j,c\}\in\mathcal{B}} \beta_{ij}^c$.

- For a given input link i and commodity c such that there exist $\{i,j,c\} \in \overline{\mathcal{B}}$, assume $\overline{\beta}_i^c > 0$, otherwise the undefined split ratios can be trivially set to 0.

- For every output link $j \in V$, define the set of input links that have an unassigned demand portion directed toward this output link, $U_j = \big\{i :\ \exists\, \{i,j,c\} \in \overline{\mathcal{B}}\big\}$.

- For a given input link i and commodity c define the set of output links, split ratios for which are to be computed, $V_i^c = \{j :\ \exists i \in U_j\}$, and assume that if nonempty, this set contains at least two elements, otherwise a single split ratio can be trivially set to $\overline{\beta}_i^c$.

- Assume that input link priorities are nonnegative, $p_i \geq 0$, $i = 1,\ldots,M$, and $\sum_{i=1}^M p_i = 1$. Note that priorities are normalized.

- Define the set of input links with zero priority: $U_{zp} = \{i :\ p_i = 0\}$. To avoid dealing with zero input priorities, perform regularization:

$$\tilde{p}_i = p_i\left(1 - \frac{|U_{zp}|}{M}\right) + \frac{1}{M}\frac{|U_{zp}|}{M} = p_i\frac{M - |U_{zp}|}{M} + \frac{|U_{zp}|}{M^2}, \tag{2.1.10}$$

  where $|U_{zp}|$ denotes the number of elements in set U_{zp}. Expression (2.1.10) implies that the regularized input priority $\tilde{p}_i$ consists of two parts: (1) the original input priority p_i normalized to the portion of input links with nonzero priorities; and (2) uniform distribution among M input links, $\frac{1}{M}$, normalized to the portion of input links with zero priorities.

  Note that $\tilde{p}_i \geq 0$, $i = 1,\ldots,M$, and $\sum_{i=1}^M \tilde{p}_i = 1$.

[1] If split ratios were undefined in this case, they could be assigned arbitrarily.

The algorithm for distributing $\overline{\beta}_i^c$ among the commodity movements in $\overline{\mathcal{B}}$, that is assigning values to the a priori unknown split ratios, aims at maintaining output links as uniformly occupied as possible. This algorithm was presented in [17] and is described next.

1. Initialize:

$$\begin{aligned}
\tilde{\beta}_{ij}^c(0) &:= \begin{cases} \beta_{ij}^c, & \text{if } \{i,j,c\} \in \mathcal{B}, \\ 0, & \text{otherwise;} \end{cases} \\
\overline{\beta}_i^c(0) &:= \overline{\beta}_i^c; \\
\tilde{U}_j(0) &= U_j; \\
\tilde{V}(0) &= V; \\
k &:= 0,
\end{aligned}$$

   Here $\tilde{U}_j(k)$ is the remaining set of input links with some unassigned demand, which may be directed to output link j; and $\tilde{V}(k)$ is the remaining set of output links, to which the still unassigned demand may be directed.

2. If $\tilde{V}(k) = \emptyset$, stop. The sought-for split ratios are $\left\{\tilde{\beta}_{ij}^c(k)\right\}$, $i = 1, \ldots, M$, $j = 1, \ldots, N$, $c = 1, \ldots, C$.

3. Calculate the remaining unallocated demand:

$$\overline{S}_i^c(k) = \overline{\beta}_i^c(k) S_i^c, \quad i = 1, \ldots, M, \;\; c = 1, \ldots, C.$$

4. For all input-output link pairs calculate oriented demand:

$$\tilde{S}_{ij}^c(k) = \tilde{\beta}_{ij}^c(k) S_i^c.$$

5. For all input-output link pairs calculate oriented priorities:

$$\tilde{p}_{ij}(k) = \tilde{p}_i \frac{\sum_{c=1}^{C} \gamma_{ij}^c S_i^c}{\sum_{c=1}^{C} S_i^c} \tag{2.1.11}$$

with

$$\gamma_{ij}^c(k) = \begin{cases} \beta_{ij}^c, & \text{if split ratio is defined a priori: } \{i,j,c\} \in \mathcal{B}, \\ \tilde{\beta}_{ij}^c(k) + \frac{\overline{\beta}_i^c(k)}{|V_i^c|}, & \text{otherwise,} \end{cases} \tag{2.1.12}$$

where $|V_i^c|$ denotes the number of elements in the set V_i^c. Comparing the expression (2.1.11)-(2.1.12) with (2.1.2), one can see that split ratios $\tilde{\beta}_{ij}^c(k)$, which are not fully defined yet, are complemented with a fraction of $\overline{\beta}_i^c(k)$ inversely proportional to the number of output links among which the flow of commodity c from input link i can be distributed.

Note that in this step we user *regularized* priorities $\tilde{p}_i$ as opposed to the original p_i, $i = 1, \ldots, M$. This is done to ensure that inputs with $p_i = 0$ are not ignored in the split ratio assignment.

6. Find the largest oriented demand-supply ratio:

$$\mu^+(k) = \max_j \max_i \frac{\sum_{c=1}^{C} \tilde{S}_{ij}^c(k)}{\tilde{p}_{ij}(k) R_j} \sum_{i \in U_j} \tilde{p}_{ij}(k).$$

7. Find the smallest oriented demand-supply ratio:

$$\mu^-(k) = \min_j \min_i \frac{\sum_{c=1}^{C} \tilde{S}_{ij}^c(k)}{\tilde{p}_{ij}(k) R_j} \sum_{i \in U_j} \tilde{p}_{ij}(k),$$

and denote i^-, j^-, input and output links, where this minimum is achieved. For details, see [17].

Define

$$c^- = \arg\min_c \overline{S}_{i^-}^c(k).$$

- If $\mu^-(k) = \mu^+(k)$, which means that the oriented demand is perfectly balanced among the

output links, distribute the unassigned demand proportionally to the allocated supply:

$$\tilde{\beta}^{c^-}_{i^-j}(k+1) = \tilde{\beta}^{c^-}_{i^-j}(k) + \frac{R_j}{\sum_{j' \in \tilde{V}^{c^-}_{i^-}(k)} R_{j'}} \overline{\beta}^{c^-}_{i^-}(k), \quad j \in \tilde{V}^{c^-}_{i^-}(k); \tag{2.1.13}$$

$$\tilde{\beta}^{c}_{ij}(k+1) = \tilde{\beta}^{c}_{ij}(k) \text{ for } \{i,j,c\} \neq \{i^-, j, c^-\}; \tag{2.1.14}$$

$$\overline{\beta}^{c^-}_{i^-}(k+1) = 0;$$

$$\overline{\beta}^{c}_{i}(k+1) = \overline{\beta}^{c}_{i}(k) \text{ for } \{i,c\} \neq \{i^-, c^-\}.$$

- Else, assign:

$$\Delta\tilde{\beta}^{c^-}_{i^-j^-}(k) = \min\left\{\overline{\beta}^{c^-}_{i^-}(k), \left(\frac{\mu^+(k)\tilde{p}_{i^-j^-}(k)R_{j^-}}{\overline{S}^{c^-}_{i^-}(k)\sum_{i\in U_{j^-}}\tilde{p}_{ij^-}(k)} - \frac{\sum_{c=1}^{C}\tilde{S}^{c}_{i^-j^-}(k)}{\overline{S}^{c^-}_{i^-}(k)}\right)\right\}; \tag{2.1.15}$$

$$\tilde{\beta}^{c^-}_{i^-j^-}(k+1) = \tilde{\beta}^{c^-}_{i^-j^-}(k) + \Delta\tilde{\beta}^{c^-}_{i^-j^-}(k); \tag{2.1.16}$$

$$\tilde{\beta}^{c}_{ij}(k+1) = \tilde{\beta}^{c}_{ij}(k) \text{ for } \{i,j,c\} \neq \{i^-, j^-, c^-\}; \tag{2.1.17}$$

$$\overline{\beta}^{c^-}_{i^-}(k+1) = \overline{\beta}^{c^-}_{i^-}(k) - \Delta\tilde{\beta}^{c^-}_{i^-j^-}(k);$$

$$\overline{\beta}^{c}_{i}(k+1) = \overline{\beta}^{c}_{i}(k) \text{ for } \{i,c\} \neq \{i^-, c^-\}.$$

8. Update sets $\tilde{U}_j(k)$ and $\tilde{V}(k)$:

$$\tilde{U}_j(k+1) = \tilde{U}_j(k) \setminus \left\{i^- : \overline{\beta}^{c}_{i^-}(k+1) = 0,\ c = 1, \ldots, C\right\}, \quad j \in \tilde{V}(k);$$

$$\tilde{V}(k+1) = \tilde{V}(k) \setminus \left\{j : \tilde{U}_j(k+1) = \emptyset\right\}.$$

9. Set $k := k+1$ and return to step 2.

This algorithm is invoked on all nodes of the road network that have a priori undefined split ratios at each time step of the LNCTM.

Inertia effect.

In its current form, that was introduced in [17], the split ratio assignment algorithm deals with input and output links without the context, which input-output pairs form unified travel facilities, e.g. HOV and general purpose (GP) lanes in a freeway as shown in Figure 2.1. Yet, taking into account

relationships between input and output links is important as it affects split ratio assignment. At decision points, such as our nodes with undefined split ratios, drivers tend to stay in the lane they are already in, unless switching promises a clear benefit — less dense traffic in the downstream link. This is called an *inertia effect*. The inertia effect can be incorporated into the split ratio assignment algorithm above: in step 5, where we assign oriented priorities, we can give higher priorities to those (i, j) pairs that belong to the same lane. The idea is to assign larger split ratios to movements that form the same lane. We shall refer to Figure 2.1 to explain the concept.

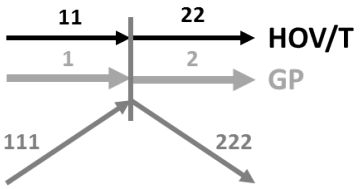

Figure 2.1: A node where some of the input links form travel facilities with some of the output links.

Here, links 1 and 2 form one travel facility (e.g., the general purpose lane), while links 11 and 22 form the other one (e.g., the HOV lane). The split ratio assignment algorithm computes the undefined split ratios with an objective of keeping traffic load of the outgoing links as balanced as possible.

Ensuring that the split ratio assignment algorithm gives preferences to movements 1-to-2 and 11-to-22 over 1-to-22 and 11-to-2 can be done in step 5, setting of oriented priorities, namely by modifying formula (2.1.12). The original formula gives us:

$$\gamma^c_{1,2}(k) = \tilde{\beta}^c_{1,2}(k) + \frac{\overline{\beta}^c_1(k)}{2} \qquad \gamma^c_{1,22}(k) = \tilde{\beta}^c_{1,22}(k) + \frac{\overline{\beta}^c_1(k)}{2};$$
$$\gamma^c_{11,2}(k) = \tilde{\beta}^c_{11,2}(k) + \frac{\overline{\beta}^c_{11}(k)}{2} \quad \gamma^c_{11,22}(k) = \tilde{\beta}^c_{11,22}(k) + \frac{\overline{\beta}^c_{11}(k)}{2}.$$

Since for $k = 0$ $\tilde{\beta}^c_{i,j}(0) = 0$, $i = 1, 11$, $j = 2, 22$, we get $\gamma^c_{1,2}(0) = \gamma^c_{1,22}(0) = \frac{\overline{\beta}^c_1(k)}{2}$ and $\gamma^c_{11,2}(0) = \gamma^c_{11,22}(0) = \frac{\overline{\beta}^c_{11}(k)}{2}$, which, according to (2.1.11), yields $\tilde{p}_{1,2}(0) = \tilde{p}_{1,22}(0)$ and $\tilde{p}_{11,2}(0) = \tilde{p}_{11,22}(0)$.

For each input link i that forms one lane with an output link $\hat{\jmath}$ and traffic commodity c, such that $\hat{\jmath} \in V_i^c$, formula (2.1.12) can be modified as follows:

$$\gamma_{ij}^c(k) = \begin{cases} \beta_{ij}^c, & \text{if split ratio is defined a priori: } \{i,j,c\} \in \mathcal{B}, \\ \tilde{\beta}_{ij}^c(k) + \overline{\beta}_i^c(k)\lambda_i^c, & i \text{ and } j \text{ form one lane: } j = \hat{\jmath}, \\ \tilde{\beta}_{ij}^c(k) + \overline{\beta}_i^c(k)\frac{1-\lambda_i^c}{|V_i^c|-1}, & i \text{ and } j \text{ are in different lanes: } j \neq \hat{\jmath}, \end{cases} \tag{2.1.18}$$

where parameter $\lambda_i^c \in \left[\frac{1}{|V_i^c|}, 1\right]$ is called the *inertia coefficient* and indicates how strong the inertia effect is. With $\lambda_i^c = \frac{1}{|V_i^c|}$, formula (2.1.18) reduces to (2.1.12). With $\lambda_i^c = 1$, all the a priori unassigned traffic from link i must stay in its lane — be directed to output link $\hat{\jmath}$. The choice of λ_i lies with the modeler. In the case of example from Figure 2.1, the modified formula (2.1.18) yields:

$$\begin{aligned} &\gamma_{1,2}^c(k) = \tilde{\beta}_{1,2}^c(k) + \overline{\beta}_1^c(k)\lambda_1^c && \gamma_{1,22}^c(k) = \tilde{\beta}_{1,22}^c(k) + \overline{\beta}_1^c(k)(1-\lambda_1^c); \\ &\gamma_{11,2}^c(k) = \tilde{\beta}_{11,2}^c(k) + \overline{\beta}_{11}^c(k)(1-\lambda_{11}^c) && \gamma_{11,22}^c(k) = \tilde{\beta}_{11,22}^c(k) + \overline{\beta}_{11}^c(k)\lambda_{11}^c, \end{aligned}$$

where $\lambda_1, \lambda_{11} \in \left[\frac{1}{2}, 1\right]$, and picking $\lambda_1 > \frac{1}{2}$ ($\lambda_{11} > \frac{1}{2}$) would give preference to movement 1-to-2 over 1-to-22 (11-to-22 over 11-to-2).

The way of choosing λ_i^c for multiple input links is not obvious and an arbitrary choice may result in the unbalanced flow distribution among output links. Therefore, we suggest picking just one input-output pair $\hat{\imath}$-to-$\hat{\jmath}$, and for that input link setting $\lambda_{\hat{\imath}}^c = 1$, while for other input links i setting $\lambda_i^c = \frac{1}{|V_i^c|}$, $c = 1, \ldots, C$. The input link $\hat{\imath}$ must be from the lane, which is expected to have positive net in-flow of vehicles as a result of split ratio assignment and the node model. So,

$$\hat{\imath} = \arg\min_{i \in \hat{U}} = \frac{\sum_{c:\{i,j,c\} \in \overline{\mathcal{B}}} \overline{S}_i^c + \sum_{i:\{i,j,c\} \in \mathcal{B}} \sum_{c:\{i,j,c\} \in \mathcal{B}} \beta_{ij}^c S_i^c}{R_j}, \tag{2.1.19}$$

where

$$\hat{U} = \{\text{input links } i : \exists j, c, \text{ s.t. } j \in V_i^c \text{ and the pair of links } (i,j) \text{ belongs to the same lane}\}, \tag{2.1.20}$$

and j denotes output link that is in the same lane as input link i.

In the context of the setting from Figure 2.1, we need to determine whether flow from link 1 will proceed to link 2 or flow from link 11 to link 22, while other a priori undefined split ratios will be computed according to the split ratio assignment algorithm. If $\hat{\imath} = 11$, then $\lambda_{11} = 1$, $\lambda_1 = \frac{1}{2}$, and a priori unassigned traffic in the HOV lane will stay in the HOV lane ($\beta^c_{11,2} = 0$), while the a priori unassigned traffic coming from links 1 and 111, will be distributed between links 2 and 22 according to the split ratio assignment algorithm.

On the other hand, if $\hat{\imath} = 1$, then $\lambda_1 = 1$, $\lambda_{11} = \frac{1}{2}$, and a priori unassigned traffic in the GP lane will stay in the GP lane ($\beta^c_{1,22} = 0$), while the a priori unassigned traffic coming from links 11 and 111, will be distributed between links 2 and 22 according to the split ratio assignment algorithm.

2.1.3 LNCTM

Each link $l \in \mathcal{L}$ is characterized by its length and the fundamental diagram, a flow-density relationship presented in Figure 2.2. A fundamental diagram is defined by four values: capacity F_l, free flow speed v_l^f, congestion wave speed w_l and the jam density n_l^J.[2]

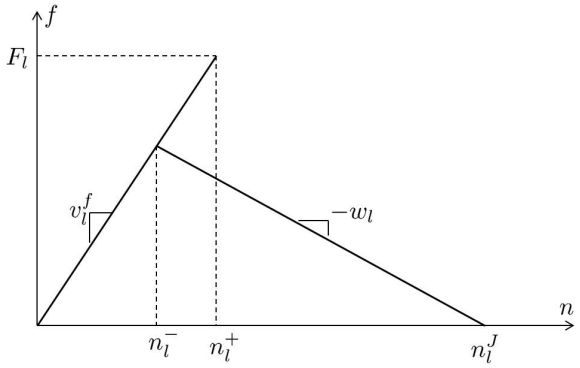

Figure 2.2: Fundamental diagram.

In this report we assume that densities, flows and speeds are *normalized* by link lengths and the discretization time step; [3] and that free flow speed v_l^f and congestion wave speed w_l satisfy the

[2]For the sake of notation, in this report we assume these values to be fixed, but in general the may be time-varyinng.

[3]Given original (not normalized) capacity $\tilde{F}_l$ specified in vehicles per hour (vph), free flow speed $\tilde{v}_l^f$ and congestion wave speed $\tilde{w}_l$ specified in miles per hour (mph), and jam density $\tilde{n}_l^J$ specified in vehicles per mile (vpm), as well as link length Δx_l and discretization time step Δt, normalized values are $F_l = \tilde{F}_l \Delta t$ specified in vehicles per time period Δt, $v_l^f = \tilde{v}_l^f \frac{\Delta t}{\Delta x_l}$ and $w_l = \tilde{w}_l \frac{\Delta t}{\Delta x_l}$, both unitless, and $n_l^J = \tilde{n}_l^J \Delta x_l$ specified in vehicles.

Courant-Friedrichs-Lewy (CFL) condition [5]: $0 \leq v_l^f, w_l \leq 1$. [4] The values $n_l^- = \frac{w_l n_l^J}{v_l^f + w_l}$ and $n_l^+ = \frac{F_l}{v_l^f}$ are called *low* and *high critical density* respectively. Unless $n_l^- = n_l^+$, when it assumes triangular shape, the fundamental diagram is not a function of density: $n_l(t) \in \left(n_l^-, n_l^+\right]$ admits two possible flow values.

Each node $\nu \in \mathcal{N}$ with M_ν input and N_ν output links is characterized by time dependent mutual restriction intervals $\{\boldsymbol{\eta}_{jj'}^i(t)\}$, input link priorities $\{p_i(t)\}$ and partially defined split ratios $\{\beta_{ij}^c(t)\}$, [5] where C is the number of vehicle types; $i = 1, \ldots, M_\nu$, $j, j' = 1, \ldots, N_\nu$ and $c = 1, \ldots, C$.

The state of the system at time t is described by the number of vehicles per commodity in each link: $\vec{n}_l(t) = \left[n_l^1(t), \ldots, n_l^C(t)\right]^T$, where $n_l^c(t)$ represents the number of vehicles of type c in link l at time t. In our notation, $n_l(t) = \sum_{c=1}^C n_l^c(t)$. The state update equation for link $l \in \mathcal{L}$ is:

$$\vec{n}_l(t+1) = \vec{n}_l(t) + \left(\vec{f}_l^{in}(t) - \vec{f}_l^{out}(t)\right), \tag{2.1.21}$$

where $\vec{f}_l^{in}(t) = \left[f_l^{1,in}(t), \ldots, f_l^{C,in}(t)\right]^T$ is the vector of commodity flows coming into link l during this time step, and $\vec{f}_l^{out}(t) = \left[f_l^{1,out}(t), \ldots, f_l^{C,out}(t)\right]^T$ is the vector of commodity flows leaving link l during this time step.

For ordinary and destination links, $\vec{f}_l^{in}(t)$ is obtained from the begin node: given a begin node ν with M_ν input links,

$$f_l^{c,in}(t) = \sum_{i=1}^{M_\nu} f_{il}^c(t), \quad c = 1, \ldots, C. \tag{2.1.22}$$

For origin links,

$$f_l^{c,in}(t) = d_l^c(t), \tag{2.1.23}$$

where $d_l^c(t)$ denotes commodity demand at time t, which is an exogenous input to the model, specified in vehicles per discretization step Δt.

[4] The CFL condition is the necessary condition for convergence while solving hyperbolic PDEs numerically.
[5] Split ratios may also be fully defined or fully undefined.

For ordinary and origin links, $\vec{f}_l^{out}(t)$ is obtained from the end node: given an end node ν with N_ν output links,

$$f_l^{c,out}(t) = \sum_{j=1}^{N_\nu} f_{lj}^c(t), \quad c = 1, \ldots, C. \tag{2.1.24}$$

For destination links,

$$f_l^{c,out}(t) = v_l^f n_l^c(t) \min\left\{1, \frac{F_l}{\sum_{c'=1}^{C} v_l^f n_l^{c'}(t)}\right\}, \quad c = 1, \ldots, C. \tag{2.1.25}$$

The values $f_{il}^c(t)$ and $f_{lj}^c(t)$ are computed by the node model from Section 2.1.1.

For each link $l \in \mathcal{L}$ we will also define a congestion metastate:

$$\theta_l(t) = \begin{cases} 0 & n_l(t) \le n_l^-, \\ 1 & n_l(t) > n_l^+, \\ \theta_l(t-1) & n_l^- < n_l(t) \le n_l^+. \end{cases} \tag{2.1.26}$$

This metastate helps determining which constraint of the fundamental diagram is activated when we compute the receive function for a link.

Now we can formally describe the LNCTM that runs for T time steps.

1. Initialize:

$$\begin{aligned} n_l^c(0) &:= n_{l,0}^c; \\ \theta_l(0) &:= \theta_{l,0}; \\ t &:= 0 \end{aligned}$$

   for all $l \in \mathcal{L}$ and $c = 1, \ldots, C$, where $n_{l,0}^c$ and $\theta_{l,0}$ are the initial conditions.

2. Apply all the control functions that modify system parameters (fundamental diagrams, input priorities) and/or system state. A control function may represent ramp metering, variable

speed limit, managed lane policy, etc. Control functions may be *open-loop* (if they depend only on time) and *closed-loop* (if they depend on time and system state). This step is optional.

3. For each link $l \in \mathcal{L}$ and commodity $c = 1, \dots, C$ define the *send* function (demand):

$$S_l^c(t) = \begin{cases} v_l^f n_l^c(t) \min\left\{1, \frac{F_l}{v_l^f \sum_{c=1}^C n_l^c(t)}\right\}, & l \text{ is an ordinary link or a destination,} \\ d_l^c(t) \min\left\{1, \frac{F_l}{\sum_{c=1}^C d_l^c(t)}\right\}, & l \text{ is an origin.} \end{cases} \tag{2.1.27}$$

4. For each link $l \in \mathcal{L}$ define the *receive* function (supply):

$$R_l(t) = \begin{cases} (1 - \theta_l(t))\, F_l + \theta_l(t) w_l \left(n_l^J - \sum_{c=1}^C n_l^c(t)\right), & l \text{ is an ordinary link or a destination,} \\ \infty, & l \text{ is an origin.} \end{cases} \tag{2.1.28}$$

5. For each node $\nu \in \mathcal{N}$ with input links $\{i\}$ and output links $\{j\}$ that has undefined split ratios, given its input link priorities $\{p_i(t)\}$, send functions $S_i^c(t)$ and receive functions $R_j(t)$, compute the undefined split ratios $\{\beta_{ij}^c(t)\}$ according to the algorithm from Section 2.1.2.

6. For each node $\nu \in \mathcal{N}$ with input links $\{i\}$ and output links $\{j\}$, given its mutual restriction intervals $\{\eta_{jj'}^i(t)\}$, input link priorities $\{p_i(t)\}$ and split ratios $\{\beta_{ij}^c(t)\}$, send functions $S_i^c(t)$ and receive functions $R_j(t)$, compute input-output flows $f_{ij}^c(t)$ according to the algorithm from Section 2.1.1.

7. For each link $l \in \mathcal{L}$, compute $\vec{f}_l^{in}(t)$ using expressions (2.1.22)-(2.1.23) and $\vec{f}_l^{out}(t)$ using expressions (2.1.24)-(2.1.25).

8. For each link $l \in \mathcal{L}$, update the state $\vec{n}_l(t+1)$ according to the conservation equation (2.1.21), and the metastate $\theta_l(t+1)$ according to its definition (2.1.26).

9. If $t = T$, then stop, otherwise set $t := t + 1$ and return to step 2.

Traffic speed for link l is computed as a ratio of total flow leaving this link to the total number of

vehicles in this link:

$$v_l(t) = \begin{cases} \frac{\sum_{c=1}^{C} f_l^{c,out}(t)}{\sum_{c=1}^{C} n_l^c(t)}, & \text{if } \sum_{c=1}^{C} n_l^c(t) > 0, \\ v_l^f, & \text{otherwise.} \end{cases} \tag{2.1.29}$$

Defined this way, $v_l(t) \in [0, v_l^f]$.

2.2 Modeling HOV Lane

We will consider two types of HOV configurations: *full access* and *separated with control access*. Full access is the configuration where the HOV lane is just another freeway lane, to (from) which eligible vehicles may switch from (to) the general purpose (GP) lane anywhere. Typically, a full access lane is designated an HOV lane only during certain periods of the day, and at other times it serves as a GP lane. On the other hand, a separated HOV lane allows traffic from and to the GP lane only at certain locations, called *gates*, and it admits only HOV traffic at all times. The implemented HOV access scheme depends on jurisdiction; for example, full access lanes are common in Northern California, and separated HOV lanes are common in Southern California. Modeling of these two configurations is described next.

2.2.1 Full Access HOV Lane

A full access HOV lane configuration is presented in Figure 2.3: GP and HOV links are parallel with the same geometry and share the same begin and end node pairs; traffic flow exchange between GP and HOV lanes can happen at every node. Links that are too long may be broken up into smaller ones by creating more nodes, such as nodes 2 and 3 in Figure 2.3. Generally, fundamental diagrams for parallel GP and HOV links are different.

We introduce two traffic commodities ($C = 2$): $c = 1$ corresponds to the low occupancy vehicle (LOV) traffic, and $c = 2$ corresponds to the HOV traffic. When HOV lane is active, $c = 1$-traffic is confined to the GP lane, whereas $c = 2$-traffic can use both GP and HOV lanes. E.g., for node 1 in

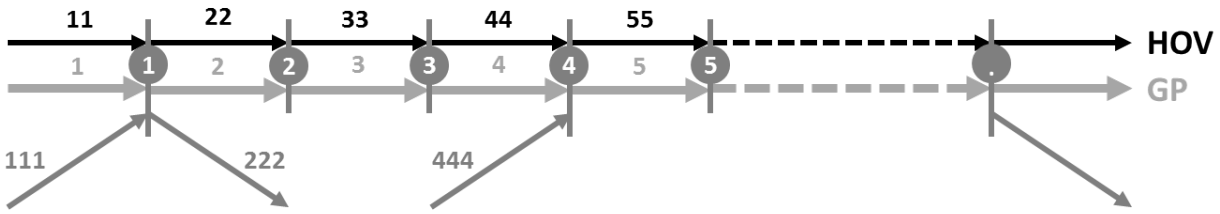

Figure 2.3: Freeway with full access HOV lane.

Figure 2.3 this policy translates to:

$$\begin{array}{llll}
\beta^1_{1,2} = 1 - \beta^1_{1,222} & \beta^1_{1,22} = 0 & \beta^1_{1,222}; & \\
\beta^1_{11,2} = 1 - \beta^1_{11,222} & \beta^1_{11,22} = 0 & \beta^1_{11,222}; & \\
\beta^1_{111,2} = 1 - \beta^1_{111,222} & \beta^1_{111,22} = 0 & \beta^1_{111,222}; & \\
\beta^2_{1,2} = \ ? & \beta^2_{1,22} = \ ? & \beta^2_{1,222} & \overline{\beta}^2_1 = 1 - \beta^2_{1,222}; \\
\beta^2_{11,2} = \ ? & \beta^2_{11,22} = \ ? & \beta^2_{11,222} & \overline{\beta}^2_{11} = 1 - \beta^2_{11,222}; \\
\beta^2_{111,2} = \ ? & \beta^2_{111,22} = \ ? & \beta^2_{111,222} & \overline{\beta}^2_{111} = 1 - \beta^2_{111,222},
\end{array} \tag{2.2.1}$$

where $\beta^c_{i,222}$, are given (for example, computed from off-ramp detector measurements), and β^2_{ij} are to be determined using the split ratio assignment algorithm from Section 2.1.2, $i = 1, 11, 111$, $j = 2, 22$. Similarly, for node 2:

$$\begin{array}{llll}
\beta^1_{2,3} = 1 & \beta^1_{2,33} = 0; & & \\
\beta^1_{22,3} = 1 & \beta^1_{22,33} = 0; & & \\
\beta^2_{2,3} = \ ? & \beta^2_{2,33} = \ ? & \overline{\beta}^2_2 = 1; & \\
\beta^2_{22,3} = \ ? & \beta^2_{22,33} = \ ? & \overline{\beta}^2_{22} = 1. &
\end{array} \tag{2.2.2}$$

When the HOV lane is deactivated and becomes available for LOV traffic, split ratios for GP and HOV output links are to be determined for both vehicle types. So, for node 1 we have:

$$\begin{array}{lll}
\beta^c_{i,j} = \ ? & \beta^c_{i,222} & \overline{\beta}^c_i = 1 - \beta^c_{i,222}; \\
i = 1, 11, 111; & j = 2, 22; & c = 1, 2;
\end{array} \tag{2.2.3}$$

and for node 2:

$$\begin{aligned} &\beta^c_{i,j} = \ ? \quad \overline{\beta}^c_i = 1; \\ &i = 2, 22; \quad j = 3, 33; \quad c = 1, 2. \end{aligned} \tag{2.2.4}$$

In this report we do not insist on any particular way of setting link priorities. One common-sense approach inspired by Tampére et al. [15] would be to make priorities proportional to link capacities, which for node 1 in Figure 2.3, will produce:

$$p_i = \frac{F_i}{F_1 + F_{11} + F_{111}}, \quad i = 1, 11, 111.$$

In some cases it makes sense to assign higher priorities to on-ramps. For example, if link 5 in Figure 2.3 has an auxiliary lane starting from node 4, which allows all (or almost all) traffic to enter freeway from on-ramp 444 even when link 5 is congested. In this situation we would set priority p_{444} proportional to $2F_{444}$. Thus, it is reasonable to set priorities of GP and HOV links proportional to their capacities, whereas on-ramp priorities depend on the configuration of the on-ramp and the freeway merging section.

Other parameters that largely depend on the freeway configuration are the mutual restriction intervals. Denote the number of sublanes[6] in links 1, 2 and 22 of Figure 2.3 L_1, L_2 and L_{22} respectively, and let $L_{1,222} < L_1$ be the number of sublanes in link 1, from which traffic can exit to the off-ramp 222. Then, one possible way of setting mutual restriction intervals would be:

$$\begin{aligned} &\boldsymbol{\eta}^i_{2,2} = [0, 1] && \boldsymbol{\eta}^i_{2,22} = \left[1 - \tfrac{1}{L_{22}}, 1\right] && \boldsymbol{\eta}^i_{2,222} = [0, 1]; \\ &\boldsymbol{\eta}^i_{22,2} = \left[0, \tfrac{1}{L_2}\right] && \boldsymbol{\eta}^i_{22,22} = [0, 1] && \boldsymbol{\eta}^i_{22,222} = [0, 0]; \\ &\boldsymbol{\eta}^i_{222,2} = \left[1 - \tfrac{L_{1,222}}{L_1}, 1\right] && \boldsymbol{\eta}^i_{222,22} = [0, 0] && \boldsymbol{\eta}^i_{222,222} = [0, 1], \end{aligned} \tag{2.2.5}$$

for all input links of node 1: $i = 1, 11, 111$. With such mutual restriction intervals we suggest that shortage of supply in GP link 2 affects the whole flow to the off-ramp 222 ($\boldsymbol{\eta}^i_{2,222} = [0, 1]$) and affects flow in one of the lanes of HOV link 22 ($\boldsymbol{\eta}^i_{2,22} = \left[1 - \tfrac{1}{L_{22}}, 1\right]$; shortage of supply in HOV link 22

[6] We use the term "sublane" here to avoid confusion with the term "lane", which throughout this report is synonymous to "facility". So, when we say that an HOV lane has 2 sublanes and a GP lane has 4 sublanes, we actually mean that the freeway has 2 HOV and 4 GP lanes.

affects flow in one of the lanes of GP link 2 ($\boldsymbol{\eta}^i_{22,2} = \left[0, \frac{1}{L_2}\right]$) and does not affect the off-ramp flow ($\boldsymbol{\eta}^i_{22,222} = [0, 0]$); shortage of supply in the off-ramp 222 affects flow in GP link 2 proportionally to the ratio of the number of lanes that send traffic to the off-ramp in link 1 to the total number of lanes in that link ($\boldsymbol{\eta}^i_{222,2} = \left[1 - \frac{L_{1,222}}{L_1}, 1\right]$) and does not affect the flow in HOV link 22 ($\boldsymbol{\eta}^i_{222,22} = [0, 0]$). A conservative alternative to this approach would be to set all mutual restriction intervals to 1, thus fully enforcing the FIFO rule.

Friction Effect

To accurately model a freeway network with full access HOV lane, we need to incorporate the so-called *friction effect* into the LNCTM: drivers' fear of moving fast in the HOV lane while traffic in the adjacent GP links moves slowly due to congestion. In other words, there should not be large speed difference between adjacent GP and HOV links, even if GP link is congested and HOV link is in free flow. This phenomenon was analyzed, among other sources, in [7]. We propose incorporating the friction effect into the step 2 of the LNCTM, applying control (see Section 2.1.3 above). This type of control is *not a traffic management technique, but an element of driver behavior modeling.* As reported in [7], if traffic in the GP lane moves slowly (due to congestion), traffic in the full access HOV lane should slow down even if it can move faster. In reality, this friction effect significantly depends on the road configuration — whether the HOV lane has one sublane or more, whether there is a shoulder lane next to the HOV lane, and, possibly, on other factors. We suggest an approach to the friction effect modeling based on a *feedback mechanism* that uses the difference of speeds in the parallel GP and HOV links to scale down the flow out of the HOV link if necessary.

To explain the concept, we again refer to Figure 2.3 and consider parallel links 1 (GP) and 11 (HOV). Recall that the link speed at a given time step t is obtained from formula (2.1.29), and assume that $v_1(t-1)$ and $v_{11}(t-1)$ are known as we perform LNCTM calculations for step $t+1$. The friction effect is present if

$$v_1(t-1) < \min\left\{v_1^f,\ v_{11}(t-1)\right\}, \tag{2.2.6}$$

which means: (1) the GP link is in congestion (its speed is below current free flow speed); and (2) the speed in the GP link is less than the speed in the HOV link.

Denote this speed differential:

$$\Delta_{11}(t) = v_{11}^f - v_1(t-1), \tag{2.2.7}$$

with $\sigma_{11} \in [0,1]$ the *friction coefficient* for the HOV link 11. The friction coefficient reflects the strength of the friction; 0 meaning there is no friction, and 1 meaning that the HOV link speed is tracking the GP link speed. Generally, the choice of the friction coefficient depends on a particular HOV lane configuration and lies with the modeler. For some specific locations, this type of analysis was done in [7].

We propose adjusting the free flow speed and the capacity of an HOV link as follows:

$$\hat{v}_l(t) = v_l^f(t) - \sigma_l \Delta_l(t); \tag{2.2.8}$$

$$\hat{F}_l(t) = \hat{v}_l(t) n_l^+, \tag{2.2.9}$$

and using these adjusted values in the calculation of the send function (2.1.27) in step 3 of the LNCTM. Thus, when friction is present in the HOV link, its send function (2.1.27) is replaced with:

$$S_l^c(t) = \begin{cases} \hat{v}_l(t) n_l^c(t) \min\left\{1, \frac{\hat{F}_l(t)}{\hat{v}_l(t)\sum_{c=1}^C n_l^c(t)}\right\}, & l \text{ is an ordinary link or a destination,} \\ d_l^c(t) \min\left\{1, \frac{\hat{F}_l(t)}{\sum_{c=1}^C d_l^c(t)}\right\}, & l \text{ is an origin.} \end{cases} \tag{2.2.10}$$

Here l represents an HOV link, and in the context of our example, $l = 11$.

For every full access HOV link l, steps 2 and 3 of the LNCTM can be summarized as follows:

1. Check if the friction effect is present: if inequality (2.2.6) does not hold, there is no friction, stop.

2. Compute adjusted free flow speed $\hat{v}_l(t)$ from (2.2.8) and adjusted capacity $\hat{F}_l(t)$ from (2.2.9).

3. If

$$\sum_{c=1}^{C} n_l^c(t) < \frac{\hat{F}_l(t)}{v_l^f - \Delta_l(t)} = \frac{\hat{v}_l(t) n_l^+(t)}{v_l^f - \Delta_l(t)}, \tag{2.2.11}$$

then use the adjusted send function (2.2.10); otherwise use the original LNCTM send function (2.1.27). Here $n_l^+(t)$ denotes high critical density (recall Figure 2.2) at time t. Condition (2.2.11) is necessary to ensure that the HOV link speed does not fall below the GP link speed of the previous time step as a result of the friction. In other words, condition (2.2.11) ensures that $v_l(t) \geq v_l^f - \Delta_l(t)$.

The case study with the full access HOV lane is presented in Chapter 3.

2.2.2 Separated HOV Lane with Control Access

The configuration of the separated HOV lane with control access is presented in Figure 2.4: GP and HOV lanes are treated as two separate freeways that have some common nodes that allow flow exchange between these two freeways. These nodes are *gates*. In the freeway with a full access HOV lane discussed previously, every node is a gate. We can disable flow exchange at a given node by fixing split ratios so that they keep traffic in its lane. For example, to disable the gate (the flow exchange between the two lanes) at node 2 in Figure 2.3, we set $\beta_{2,3}^c = 1$ and $\beta_{22,33}^c = 1$ ($\beta_{2,33}^c = 0$ and $\beta_{22,3}^c = 0$), $c = 1, 2$. Thus, the full access HOV lane can be easily converted into the separated HOV lane by fixing split ratios everywhere but designated gate-nodes. In practice, a gate is stretch of freeway about 0.5 miles long, and, potentially, we can designate two or three nodes in a row as gates. However, we assume that a gate is a single node.

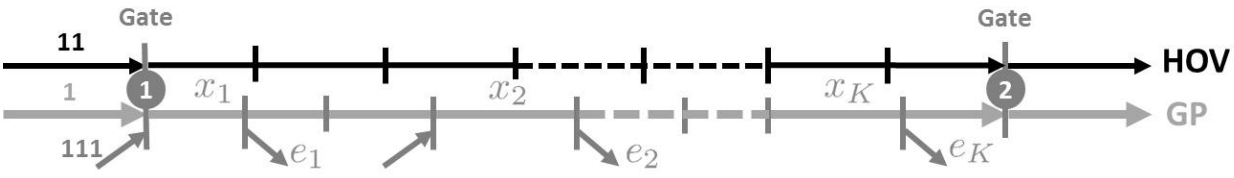

Figure 2.4: Freeway with separated HOV lane and gates.

For the separated HOV configuration, we suggest setting mutual restriction coefficients just as in the case of full access HOV lane, according to formula (2.2.5).

Contrary to the full access HOV lane, however, the separated HOV lane has a mitigated friction effect [8]: drivers in the separated HOV lane feel somewhat protected by the buffer, whether it is virtual (double solid line) or real (concrete), from vehicles changing abruptly from the slow moving GP lane and, therefore, do not drop speed as dramatically. The degree to which the friction effect is mitigated is disputed (see for example Footnote 3 in [4]), but overall the bottlenecks created by the gates are much greater instigators of congestion [4]. Inclusion of the friction effect in modeling separated HOV lane configurations is thus not as essential as in modeling the full access case.

Directing Traffic from the HOV Lane to Off-Ramps

In the full access HOV model, we could direct traffic from the HOV lane to off-ramps by setting corresponding split ratios, e.g. $\beta^c_{11,222}$, $c = 1, 2$, for node 1 in configuration from Figure 2.3. The challenge of the separated HOV lane modeling is that generally gates do not coincide with off-ramp locations. Typically, there are between 2 and 5 off-ramps in the freeway segment from one gate to the next. Off-ramps in the GP road segment connecting two gates in Figure 2.4 are identified as exits $e_1, e_2, \ldots, e_K$, and they cannot be accessed directly from the HOV lane. Vehicles traveling in the HOV lane that intend to take one of the exits $e_1, \ldots, e_K$, must switch from the HOV lane to the GP lane at gate-node 1 and then be directed to the correct off-ramp.

To resolve this challenge, we introduce new traffic commodities in addition to already existing $c = 1$ (LOVs) and $c = 2$ (HOVs) that were introduced in the full access HOV lane model, Section 2.2.1. These additional commodities will be used to distinguish traffic by its destination off-ramp. Assuming that K is the largest number of off-ramps in the GP lane between two adjacent gates, altogether we have $C = K + 2$ traffic commodities: $c = 1, 2, e_1, \ldots, e_K$, where e_k indicates the destination off-ramp in reference to Figure 2.4. By definition, traffic of type $c = e_k$ *may exist* in the GP lane segment between gate 1 and off-ramp e_k, but there is *no traffic of this type* either in the GP lane segment between off-ramp e_k and gate 2 or in the HOV lane. To ensure this, we set *constant* split

ratios:

$$\begin{aligned}
&\beta^{e_k}_{i,x_1} = 1, \quad i = 1, 11, 111, && \text{direct all } e_k\text{-type traffic to the GP lane at gate 1;} \\
&\beta^{e_k}_{x_k,e_k} = 1, && \text{direct all } e_k\text{-type traffic to off-ramp } e_k; \\
&\beta^{e_k}_{x_{k'},e_{k'}} = 0, \quad k' \neq k, && \text{do not send any } e_k\text{-type traffic to other off-ramps,}
\end{aligned} \tag{2.2.12}$$

where $k = 1, \ldots, K$, and x_k denotes the input GP link for the node that has the output link e_k (see Figure 2.4).

Now we explain how e_k-type traffic appears in the system. The original demand $d^c_l(\cdot)$ is specified at origin links l for commodities $c = 1, 2$, and $d^{e_k}_l(\cdot) \equiv 0$, $k = 1, \ldots, K$. Destination specific traffic appears in the HOV links that end at gate-nodes by assigning destinations to portions of the type-1 (LOV) and type-2 (HOV) traffic in those links. We propose incorporating this destination assignment into the step 2 of the LNCTM, applying control (Section 2.1.3) and using off-ramp split ratios $\beta^c_{x_k,e_k}$, $c = 1, 2$, $k = 1, \ldots, K$, to determine portions of HOV lane traffic to be assigned particular destinations. The destination assignment algorithm at a given time t, for a given HOV link ending with a gate-node, is described next. Without the loss of generality, we will refer to Figure 2.4 and the HOV link 11 ending at the gate-node 1 in this description.

1. Given are vehicle counts per commodity n^c_{11}, $c = 1, 2, e_1, \ldots, e_K$; free flow speed v_{11}; and off-ramp split ratios $\beta^1_{x_k,e_k}$ and $\beta^2_{x_k,e_k}$, $k = 1, \ldots, K$.[7]

2. Initialize:

$$\begin{aligned}
\tilde{n}^c_{11}(0) &:= n^c_{11}, \quad c = 1, 2, e_1, \ldots e_K; \\
k &:= 1.
\end{aligned}$$

[7] If a given GP segment connecting two adjacent gates has K' off-ramps, where $K' < K$, then assume $\beta^1_{x_k,e_k} = \beta^2_{x_k,e_k} = 0$ for $k \in (K', K]$.

3. Assign e_k-type traffic:

$$\tilde{n}_{11}^{e_k}(k) = \tilde{n}_{11}^{e_k}(k-1) + \beta_{x_k,e_k}^1 v_{11}\tilde{n}_{11}^1(k-1) + \beta_{x_k,e_k}^2 v_{11}\tilde{n}_{11}^2(k-1); \quad (2.2.13)$$

$$\tilde{n}_{11}^1(k) = \tilde{n}_{11}^1(k-1) - \beta_{x_k,e_k}^1 v_{11}\tilde{n}_{11}^1(k-1); \quad (2.2.14)$$

$$\tilde{n}_{11}^2(k) = \tilde{n}_{11}^2(k-1) - \beta_{x_k,e_k}^2 v_{11}\tilde{n}_{11}^2(k-1). \quad (2.2.15)$$

4. If $k < K$, then set $k := k + 1$ and return to step 3.

5. Update the state:

$$n_{11}^c = \tilde{n}_{11}^c(K), \quad c = 1, 2, e_1, \ldots, e_K.$$

The case study with the separated HOV lane is presented in Chapter 4.

2.3 Modeling HOT Lane

To extend the proposed full access and gated HOV lane models to HOT, we introduce new vehicle class — *LOVs that are ready to pay* — following the notation of Section 2.2.1, $c = 3$. Just as $c = 2$-traffic, $c = 3$-traffic can use both GP and HOT lanes. E.g., for node 1 in Figure 2.1 this policy translates to:

$$\begin{array}{llll}
\beta_{1,2}^1 = 1 - \beta_{1,222}^1 & \beta_{1,22}^1 = 0 & \beta_{1,222}^1; & \\
\beta_{11,2}^1 = 1 - \beta_{11,222}^1 & \beta_{11,22}^1 = 0 & \beta_{11,222}^1; & \\
\beta_{111,2}^1 = 1 - \beta_{111,222}^1 & \beta_{111,22}^1 = 0 & \beta_{111,222}^1; & \\
\beta_{1,2}^2 = \ ? & \beta_{1,22}^2 = \ ? & \beta_{1,222}^2 & \overline{\beta}_1^2 = 1 - \beta_{1,222}^2; \\
\beta_{11,2}^2 = \ ? & \beta_{11,22}^2 = \ ? & \beta_{11,222}^2 & \overline{\beta}_{11}^2 = 1 - \beta_{11,222}^2; \\
\beta_{111,2}^2 = \ ? & \beta_{111,22}^2 = \ ? & \beta_{111,222}^2 & \overline{\beta}_{111}^2 = 1 - \beta_{111,222}^2, \\
\beta_{1,2}^3 = \ ? & \beta_{1,22}^3 = \ ? & \beta_{1,222}^3 & \overline{\beta}_1^3 = 1 - \beta_{1,222}^3; \\
\beta_{11,2}^3 = \ ? & \beta_{11,22}^3 = \ ? & \beta_{11,222}^3 & \overline{\beta}_{11}^3 = 1 - \beta_{11,222}^3; \\
\beta_{111,2}^3 = \ ? & \beta_{111,22}^3 = \ ? & \beta_{111,222}^3 & \overline{\beta}_{111}^3 = 1 - \beta_{111,222}^3,
\end{array} \quad (2.3.1)$$

where $\beta^c_{i,222}$, are given (for example, computed from off-ramp detector measurements), and β^c_{ij} are to be determined using the split ratio assignment algorithm from Section 2.1.2, $i = 1, 11, 111$, $j = 2, 22$, $c = 2, 3$. Thus, we will deal with $C = 3$, in the case of full access HOT lane, and with $C = K + 3$, in the case of gated HOT lane, traffic commodities.

The other component of the HOT model is the HOT controller consisting of two parts:

1. Calculation of the toll based on the vehicle flow in the HOT lane; and
2. Calculation of the portion of LOVs ready to pay given toll and reassigning vehicles between classes $c = 1$ and $c = 3$ accordingly.

Toll $\pi(\cdot)$ varies between its minimal and maximal values, $\pi_{\min}$ and $\pi_{\max}$, and is computed from the *flow-price curve*, depicted in Figure 2.5, where f^{in}_{22} denotes total flow entering link 22 in Figure 2.1. The flow-price curve is defined by the HOT lane operator in the form of lookup table.

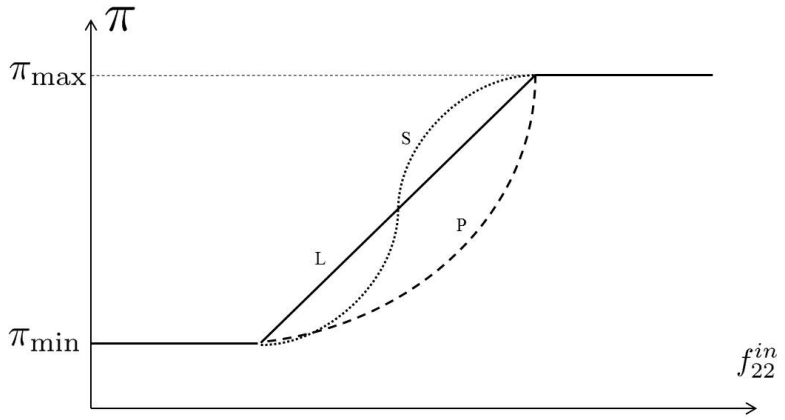

Figure 2.5: Flow-price curve: toll depends on the total flow entering the HOT link (link 22, as in Figure 2.1). Shown are linear (L), polynomial (P) and sigmoid (S) dependencies.

In the second part of the HOT controller we should determine the portion of LOVs ready to pay given price for using HOT lane. The readiess to pay may depend on multiple factors, most obvious of which are:

1. Toll value;
2. Difference in traffic density between GP and HOT lanes;

3. The estimated gain in travel time of the HOT lane over the GP lane; and

4. Travel time reliability.

In this project, we coonsidered readiness to pay depending on items 1 and 2 — toll value and the difference between the GP and the HOT traffic densities.[8]

Using the link numeration from Figure 2.1, the portion $\rho(t)$ of LOVs ready to pay toll $\pi\left(f_{22}^{in}(t)\right)$ in link 1 at time t is:

$$\rho(t) = \frac{1}{1+e^{-z(t)}}, \quad \text{where } z(t) = \alpha_0 + \alpha_1 \sum_{c=1}^{C} \left(\frac{n_2^c(t)}{L_2} - \frac{n_{22}^c(t)}{L_{22}} \right) + \alpha_2 \pi\left(f_{22}^{in}(t)\right). \tag{2.3.2}$$

Here, $n_2^c(t)$, $n_{22}^c(t)$ are the vehicle counts in links 2 and 22 from Figure 2.1, respectivly; L_2, L_{22} are lane counts in those links; and $\alpha_0, \alpha_1, \alpha_2$ are known coefficients determined through calibration of the HOT controller (see Section 2.4).

Given the vehicle counts per commodity $n_1^c(t)$ and $n_{111}^c(t)$, $c = 1 \ldots, C$, and the portion of LOVs ready to pay $\rho(t)$, the HOT controller adjusts commodity counts as follows:

$$\tilde{n}_1^1(t) = (1-\rho(t))\left(n_1^1(t) + n_1^3(t)\right), \qquad \tilde{n}_1^3(t) = \rho(t)\left(n_1^1(t) + n_1^3(t)\right); \tag{2.3.3}$$

$$\tilde{n}_{111}^1(t) = (1-\rho(t))\left(n_{111}^1(t) + n_{111}^3(t)\right), \quad \tilde{n}_{111}^3(t) = \rho(t)\left(n_{111}^1(t) + n_{111}^3(t)\right). \tag{2.3.4}$$

Here, the link IDs refer to the configuration in Figure 2.1. We do not adjust commodities in the HOT link 11, because only ready to pay LOVs may be there.[9]

Now we can summarize the action of the HOT controller:

1. Determine toll π from the flow-price curve in Figure 2.5.

[8] We did not include travel time and travel time reliability, because the analysis of I-10 East and West HOT lane data showed that there are always paying LOVs in the HOT lane, even during time periods when GP lane is *always* in free flow.

[9] Existing HOT policies are such that once a vehicle enters the HOT lane, its toll is set, and it is guaranteed that the driver would not be charged more than that. Thus, we can assume that those LOVs that were ready to pay and ended up in the HOT lane will stay ready to pay.

2. Compute $\rho(t)$ using formula (2.3.2).

3. Adjust commodity counts using formulae (2.3.3)-(2.3.4).

The HOT controller works on all GP links and on-ramps whose end node is a gate (in full access configuration, every node is a gate). This controller is activated in the step 2 of the LNCTM (see Section 2.1.3). Not all ready to pay vehicles end up in the HOT lane, but only those assigned to it in step 5 (split ratio assignment) of the LNCTM.

2.4 Calibration of HOT Controller

To compute coefficients $\alpha_0, \alpha_1, \alpha_2$ for the formula (2.3.2), we make the following assumptions:

1. We can count vehicles in the GP lane, $\hat{n}^t_{GP}$, and in the HOT lane, $\hat{n}^t_{HOT}$ at any given time t.

2. We have data to estimate the LOV traffic portion ready to pay at time t, $\hat{\rho}^t$:

$$\hat{\rho}^t = \frac{\text{Number of LOVs in the HOT link at time } t}{\text{Total number of LOVs in both HOT and GP links at time } t}. \tag{2.4.1}$$

   The nominator in the right hand side of this formula comes from FasTrak data collected in the HOT lane — if the vehicle pays, it is LOV, otherwise it is HOV. The denominator in the right hand side of this formula is computed as a sum of vehicle count in the GP lane, which can be obtained from PeMS [3], and the number of LOVs in the HOT lane. Obviously, $\hat{\rho} \in [0, 1]$.

3. We know HOT price per mile at time t, π^t, which comes from the FasTrak toll logs.

4. If traffic density per lane in the GP and the HOT lanes were the same and no tolls were collected, we assume the readiness to pay $\rho = \frac{L_{HOT}}{L_{GP}+L_{HOT}}$, where L_{GP} and L_{HOT} denote lane counts in GP and HOT links (links 2 and 22 from Figure 2.1 respectively). According to (2.3.2),

$$\rho = \frac{1}{1+e^{-\alpha_0}} = \frac{e^{\alpha_0}}{1+e^{\alpha_0}} = \frac{L_{HOT}}{L_{GP}+L_{HOT}}. \tag{2.4.2}$$

Hence,

$$\alpha_0 = \ln\left(\frac{\rho}{1-\rho}\right) = \ln\left(\frac{L_{HOT}}{L_{GP}}\right). \tag{2.4.3}$$

Thus, it remains to determine coefficients α_1 and α_2.

We will estimate α_1, α_2 from equations:

$$\ln\left(\frac{\hat{\rho}^t}{1-\hat{\rho}^t}\right) = \ln\left(\frac{L_{HOT}}{L_{GP}}\right) + \alpha_1\left(\frac{\hat{n}^t_{GP}}{L_{GP}} - \frac{\hat{n}^t_{HOT}}{L_{HOT}}\right) + \alpha_2\pi^t, \quad t = 1, \ldots, \Theta. \tag{2.4.4}$$

Denote:

$$\boldsymbol{X} = \begin{pmatrix} \frac{\hat{n}^1_{GP}}{L_{GP}} - \frac{\hat{n}^1_{HOT}}{L_{HOT}} & \pi^1 \\ \cdots & \cdots \\ \frac{\hat{n}^\Theta_{GP}}{L_{GP}} - \frac{\hat{n}^\Theta_{HOT}}{L_{HOT}} & \pi^\Theta \end{pmatrix}, \quad \text{and} \quad \boldsymbol{Y} = \begin{pmatrix} \ln\left(\frac{\hat{\rho}^1}{1-\hat{\rho}^1}\right) - \ln\left(\frac{L_{HOT}}{L_{GP}}\right) \\ \vdots \\ \ln\left(\frac{\hat{\rho}^\Theta}{1-\hat{\rho}^\Theta}\right) - \ln\left(\frac{L_{HOT}}{L_{GP}}\right) \end{pmatrix}. \tag{2.4.5}$$

Equations (2.4.4) can be rewritten as:

$$\boldsymbol{Y} = \boldsymbol{X}\begin{pmatrix} \alpha_1 \\ \alpha_2 \end{pmatrix}. \tag{2.4.6}$$

Thus, α_1, α_2 can be estimated using the least squares method:

$$\begin{pmatrix} \alpha_1 \\ \alpha_2 \end{pmatrix} = \left(\boldsymbol{X}^T\boldsymbol{X}\right)^{-1}\boldsymbol{X}^T\boldsymbol{Y}. \tag{2.4.7}$$

In Chapter 5 we present calibration of the HOT controller using data from I10 West HOT lane.

2.5 Model Calibration

When it comes to the simulation of real world traffic networks, in our case freeways with HOV/T lanes, the quality of the simulation results is assessed by comparing them with detector measurements. We expect to have flow and speed measurements at the freeway mainline (from both GP and HOV/T lanes), as well as flow measurements at on- and off-ramps. To better match the detector measurements the simulation model needs to be tuned. Tunable parameters of our model are:

- Fundamental diagram parameters, free flow speed v_l, congestion wave speed w_l, capacity F_l and the jam density n_l^J, for each link. Calibration of the fundamental diagram is typically model-agnostic, and there exists an abundant research on this topic, including from some of the authors of this report, e.g. [6]. So, we shall assume that this problem is solved.

- Percentage of high-occupancy vehicles in the traffic flow entering the system. This parameter depends on the time of day and location as well as on the type of HOV/T lane.[10] It could be roughly estimated as a ratio of the HOV lane vehicle count to the total freeway vehicle count during periods of congestion at any given location.

- Inertia coefficients. These parameters affect only how traffic of different classes mixes in different links, but they have no effect on the total vehicle counts produced by the simulation. For setting the inertia coefficients, we suggest the approach described in the second part of the Section 2.1.2.

- Friction coefficients. How to tune these parameters is an open question. In [7] the dependency of the HOV/T lane speed on the GP lane speed was investigated under different occupancy of the HOV/T lane, and the presented data suggests that although the correlation between the two speeds exists, it is not very strong, below 0.4. Therefore, we suggest setting friction coefficients to values not exceeding 0.4.

- Mutual restriction intervals. It is also an open question how to estimate mutual restriction intervals from the measurement data. We suggest using expression (2.2.5) as a default guideline.

[10] Typical minimum vehicle occupancy level for HOV lanes in the U.S. is 2 (2+HOV) or sometimes 3 (3+HOV).

- Off-ramp split ratios. The focus of this Section will be on computing these split ratios given known off-ramp flows.

2.5.1 Split Ratios for the Full Access HOV/T Lane

Consider a node, one of whose output links is an off-ramp, depicted in Figure 2.1. We shall make the following assumptions.

1. Total flow entering the off-ramp, $\hat{f}^{in}_{222}$, at any given time is known (from measurements) and is not restricted by the off-ramp supply: $\hat{f}^{in}_{222} < R_{222}$.
2. Portions of traffic sent to the off-ramp from the HOV/T lane and from the GP lane at any given time are equal: $\beta^c_{1,222} = \beta^c_{11,222} = \beta$, $c = 1, \ldots, C$.
3. None of the flow coming from the on-ramp (link 111), if such flow exists, is directed toward the off-ramp. In other words, $\beta^c_{111,222} = 0$, $c = 1, \ldots, C$.
4. Distribution of flow portions not directed to the off-ramp between the HOV/T and the GP output links is known. This can be written as: $\beta^c_{ij} = (1-\beta)\delta^c_{ij}$, where $\delta^c_{ij} \in [0,1]$, as well as $\beta_{111,j}$, $i = 1, 11$, $j = 2, 22$, $c = 1, \ldots, C$, are known.
5. Demand S^c_i, $i = 1, 11, 111$, $c = 1, \ldots, C$, and supply R_j, $j = 2, 22$, are given.

At any given time, β is unknown and is to be found.

If β were known, the node model described in Section 2.1.1, would compute the input-output flows, in particular, $f_{i,222} = \sum_{c=1}^{C} f^c_{i,222}$, $i = 1, 11$. Define

$$\psi(\beta) = f_{1,222} + f_{11,222} - \hat{f}^{in}_{222}. \tag{2.5.1}$$

Our goal is to find β from the equation:

$$\psi(\beta) = 0, \tag{2.5.2}$$

such that $\beta \in \left[\frac{\hat{f}_{222}^{in}}{S_1+S_{11}}, 1\right]$, where $S_i = \sum_{c=1}^{C} S_i^c$. Obviously, if $S_1 + S_{11} < \hat{f}_{222}^{in}$, the solution does not exist, and the best we can do in this case, is to set $\beta = 1$ directing all traffic from links 1 and 11 to the off-ramp.

Suppose now that $S_1 + S_{11} >= \hat{f}_{222}^{in}$. For any given $\hat{f}_{222}^{in}$, $\psi(\beta)$ is a monotonically increasing function of β. Moreover, $\psi\left(\frac{\hat{f}_{222}^{in}}{S_1+S_{11}}\right) \leq 0$, while $\psi(1) \geq 0$. Thus, the solution of (2.5.2) within given interval exists and can be obtained using the *bisection method*.

The algorithm for finding β follows.

1. Initialize:

$$\begin{aligned} \underline{b}(0) &:= \frac{\hat{f}_{222}^{in}}{S_1 + S_{11}}; \\ \overline{b}(0) &:= 1; \\ k &:= 0. \end{aligned}$$

2. If $S_1 + S_{11} \leq \hat{f}_{222}^{in}$, then set $\beta = 1$ and stop.

3. Run the node model from Section 2.1.1 with $\beta = \underline{b}(0)$ and evaluate $\psi(\beta)$. If $\psi(\underline{b}(0)) \geq 0$, then set $\beta = \underline{b}(0)$ and stop.

4. Run the node model from Section 2.1.1 with $\beta = \frac{\underline{b}(k)+\overline{b}(k)}{2}$ and evaluate $\psi(\beta)$. If $\psi\left(\frac{\underline{b}(k)+\overline{b}(k)}{2}\right) = 0$, then set $\beta = \frac{\underline{b}(k)+\overline{b}(k)}{2}$ and stop.

5. If $\psi\left(\frac{\underline{b}(k)+\overline{b}(k)}{2}\right) < 0$, then update:

$$\begin{aligned} \underline{b}(k+1) &= \frac{\underline{b}(k) + \overline{b}(k)}{2}; \\ \overline{b}(k+1) &= \overline{b}(k). \end{aligned}$$

Else, update:

$$\begin{aligned} \underline{b}(k+1) &= \underline{b}(k); \\ \overline{b}(k+1) &= \frac{\underline{b}(k)+\overline{b}(k)}{2}. \end{aligned}$$

6. Set $k := k+1$ and return to step 4.

2.5.2 Split Ratios for the Separated HOV/T Lane

The configuration of a node with an off-ramp as one of the output links is simpler in the case of a separated HOV/T lane, as shown in Figure 2.6. Here, traffic cannot directly go from the HOV/T lane to link 222, and, thus, we have to deal only with the 2-input-2-output node. There is a caveat, however. Recall from Section 2.2.2 that in the separate HOV/T lane case we have destination-based traffic commodities, and split ratios for destination-based traffic are fixed.

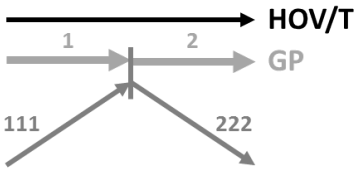

Figure 2.6: A node with a GP link and an on-ramp as inputs, and a GP link and an off-ramp as outputs.

We shall make the following assumptions:

1. Total flow entering the off-ramp, $\hat{f}^{in}_{222}$, at any given time is known (from measurements) and is not restricted by the off-ramp supply: $\hat{f}^{in}_{222} < R_{222}$.

2. All the flow coming from the on-ramp (link 111), if such flow exists, is directed toward the GP link 2. In other words, $\beta^c_{111,2} = 1$ and $\beta^c_{111,222} = 0$, $c = 1, \ldots, C$.

3. Demand S^c_i, $i = 1, 111$, $c = 1, \ldots, C$, and supply R_2 are given.

4. Denote the set of destination-based commodities as $\mathcal{D}$. Split ratios β^c_{1j} for $c \in \mathcal{D}$ are known. Split ratios $\beta^c_{1j} = \beta$ for $c \in \overline{\mathcal{D}}$, where β is to be determined.

The first three assumptions here reproduce assumptions 1, 3 and 5 made for the full access HOV/T lane case. Assumption 4 is a reminder that there is a portion of traffic flow that we cannot direct to or away from the off-ramp, but we have to account for it.

Similarly to the full access HOV/T case, define function $\psi(\beta)$:

$$\psi(\beta) = \sum_{c \in \overline{\mathcal{D}}} f^c_{1,222} + \sum_{c \in \mathcal{D}} f^c_{1,222} - \hat{f}^{in}_{222}, \tag{2.5.3}$$

where $f^c_{1,222}$, $c = 1, \ldots, C$ are determined by the node model from Section 2.1.1. The first term of the right-hand sight of (2.5.3) depends on β. As before, $\psi(\beta)$ is a monotonically increasing function. We look for the solution of equation (2.5.2) on the interval $[0, 1]$. This solution exists iff $\psi(0) \leq 0$ and $\psi(1) \geq 0$. The algorithm for finding β is the same as the one presented in the previous section, except that $\underline{b}(0)$ should be initialized to 0, and S_{11} is to be assumed 0.

2.5.3 Overview of the Calibration Process

The model calibration follows the workflow diagram shown in Figure 2.7.

1. We start by assembling the available measurement data. Fundamental diagrams are assumed to be given. Mainline and on-ramp demand is specified per 5-minute periods together with the HOV portion parameter indicating the fraction of the input demand that is HOV. Initially we do not know off-ramp split ratios as they cannot be measured directly. So we use some arbitrary values to represent them and call it "initially guessed off-ramp split ratios". What can be measured instead of off-ramp split ratios, are the flows directed to off-ramps, to which we refer to as *off-ramp demand*. Finally, if we model the HOT lane, we need the readiness to pay coefficients $\alpha_0, \alpha_1, \alpha_2$ for equation (2.3.2), obtained as descibed in Section 2.5.

2. We run LNCTM model as described in Section 2.1.3, where in step 5 the a priori undefined split ratios between traffic in the GP and in the HOV/T lanes (see expressions (2.2.1) and (2.3.1)) will be assigned.

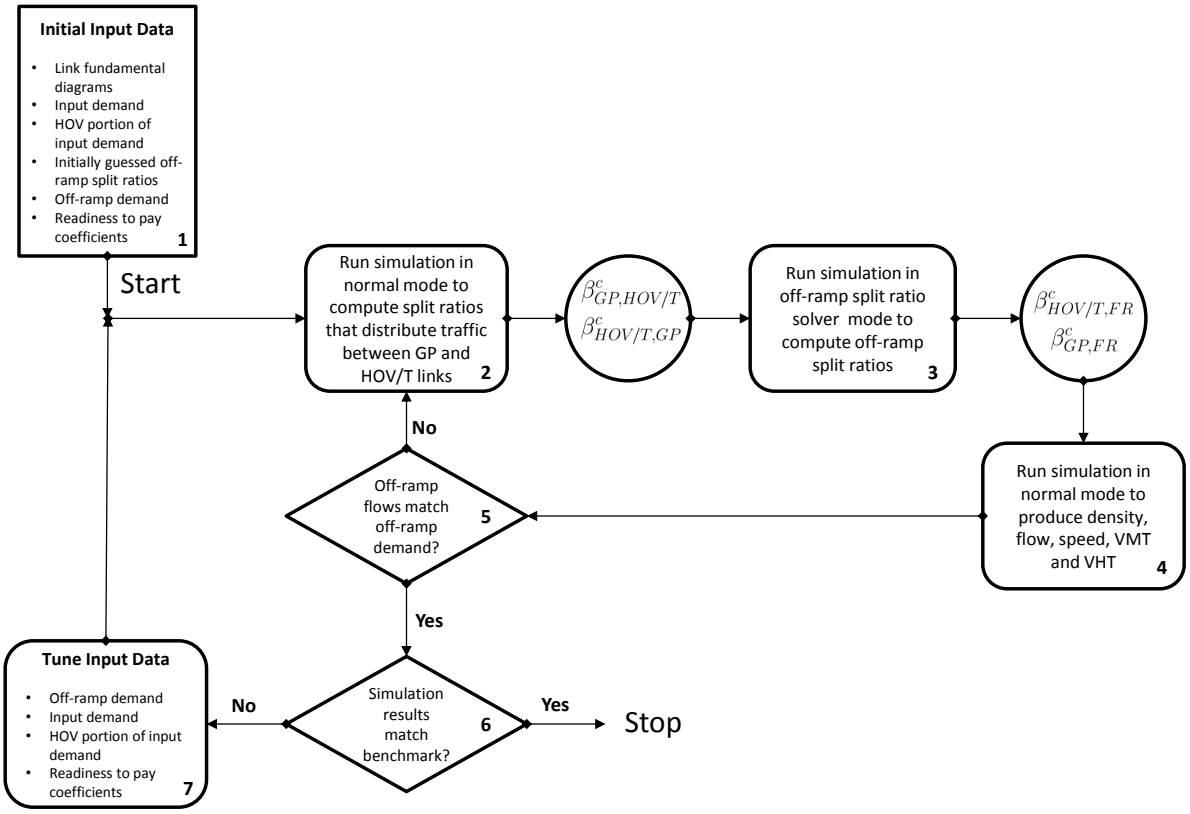

Figure 2.7: Calibration workflow.

3. Using these newly assigned split ratios we run the LNCTM model again, only this time, instead of using given off-ramp split ratios, we compute them from the given off-ramp demand as described in Sections 2.5.1 and 2.5.2. As a result of this step, we obtain new off-ramp split ratios.

4. Now we run the LNCTM model as we did originally, in step 2, only this time with new off-ramp split ratios, and record the simulation results — density, flow, speed, as well as performance measures such as vehicle miles traveled (VMT) and vehicle hours traveled (VHT).

5. Check if the resulting off-ramp flows match the off-ramp demand. If yes, proceed to step 6, otherwise, repeat steps 2-5. Usually, it takes the process described in steps 2-5 no more than two iterations to converge.

6. Evaluate the simulation results:

- correctness of bottleneck locations and activation times;
- correctness of congestion extension at each bottleneck;
- correctness of VMT and VHT.

If the simulation results are satisfactory, stop. Otherwise, proceed to step 7.

7. Tune input data in the order shown in block 7 of Figure 2.7.

Chapter 3

Full Access HOV Lane: I-680 North

We consider a 26.8-mile stretch of I-680 North freeway in Contra Costa County from postmile 30 to postmile 56.8, shown in Figure 3.1, as a test case for the full access HOV lane configuration. This freeway stretch contains two HOV lane segments whose begin and end points are marked on the map. The first HOV segment is 12.3 miles long and will be converted to HOT in spring 2017 [13], and the second HOV segment is 4.5 miles long. There are 26 on-ramps and 24 off-ramps. The HOV lane is active from 5 to 9 am and from 3 to 7 pm. The rest of the time the HOV lane behaves as a GP lane.

To build the model, we used data collected for the I-680 Corridor System Management Plan (CSMP) study [14]. The bottleneck locations as well as their activation times and congestion extension were identified in that study using video monitoring and tachometer vehicle runs. On- and off-ramp flows were given in 5-minute increments. Here we assume that HOV portion of the input demand is 15%. The model was calibrated to a *typical weekday*, as suggested in the I-680 CSMP study.

Fundamental diagrams were assigned as follows:

- Capacity of the ordinary GP lane is 1,900 vphl;
- Capacity of the auxiliary GP lane is 1,900 vphl;
- Capacity of HOV lane is 1,800 vphl while active and 1,900 vphl when it behaves as a GP lane;

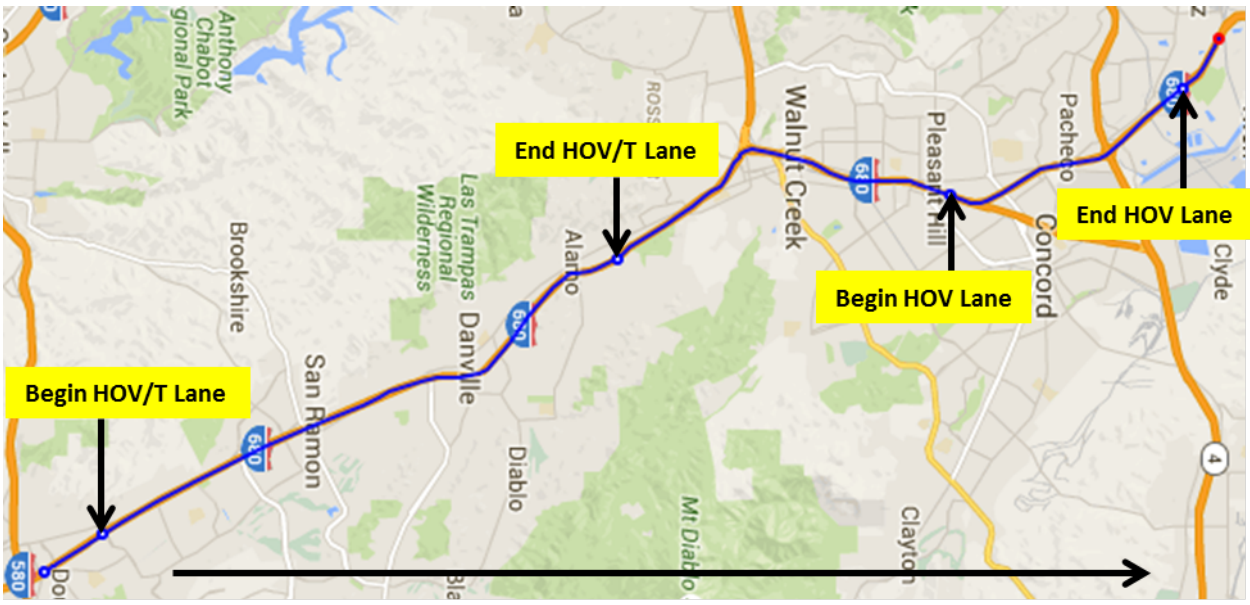

Figure 3.1: Map of I-680 North in Contra Costa County.

- Free flow speed varies between 63 and 70 mph — its measurements came partially from PeMS [3] and partially from tachometer vehicle runs.
- Congestion wave speed for each link was taken as 1/5 of the free flow speed.

The modeling results are presented in Figures 3.2, 3.3 and 3.4 showing speed, density and flow contours in the GP and the HOV lanes respectively. Each of these plots consists of the top, corresponding to the HOV lane, and bottom, corresponding to the GP lane, parts. In all the plots traffic moves from left to right along the "Absolute Postmile" axis, while the vertical axis represents time. Bottleneck locations and congestion areas identified by the I-680 CSMP study are marked by blue boxes in GP lane contours. HOV lane does not get congested, but there is a speed drop due to the *friction effect*. The friction effect, when vehicles in the HOV lane slow down because of the slow moving GP lane traffic, can be seen in the HOV lane speed contour in Figure 3.2.

Figure 3.5 shows an example of how well the off-ramp flow computed by the simulation matches the target, referred to as *off-ramp demand*, taken from the off-ramp at Crow Canyon Road. We can see that in the beginning and in the end of the day the computed flow falls below the target (corresponding areas are marked with red circles). This is due to the shortage of the mainline traffic — the off-ramp demand cannot be satisfied.

Finally, Table 3.1 summarizes the performance measurements — vehicle miles traveled (VMT), vehicle hours traveled (VHT) and delay in vehicle-hours — computed by simulation versus collected in the course of the I-680 CSMP study. Delay is computed for vehicles with speed below 45 mph.

	Simulation result	Collected data
GP Lane VMT	1,687,618	-
HOV Lane VMT	206,532	-
Total VMT	1,894,150	1,888,885
GP Lane VHT	27,732	-
HOV Lane VHT	3,051	-
Total VHT	30,783	31,008
GP Lane Delay	2,785	-
HOV Lane Delay	6	-
Total Delay	2,791	2,904

Table 3.1: Performance measures for I-680 North.

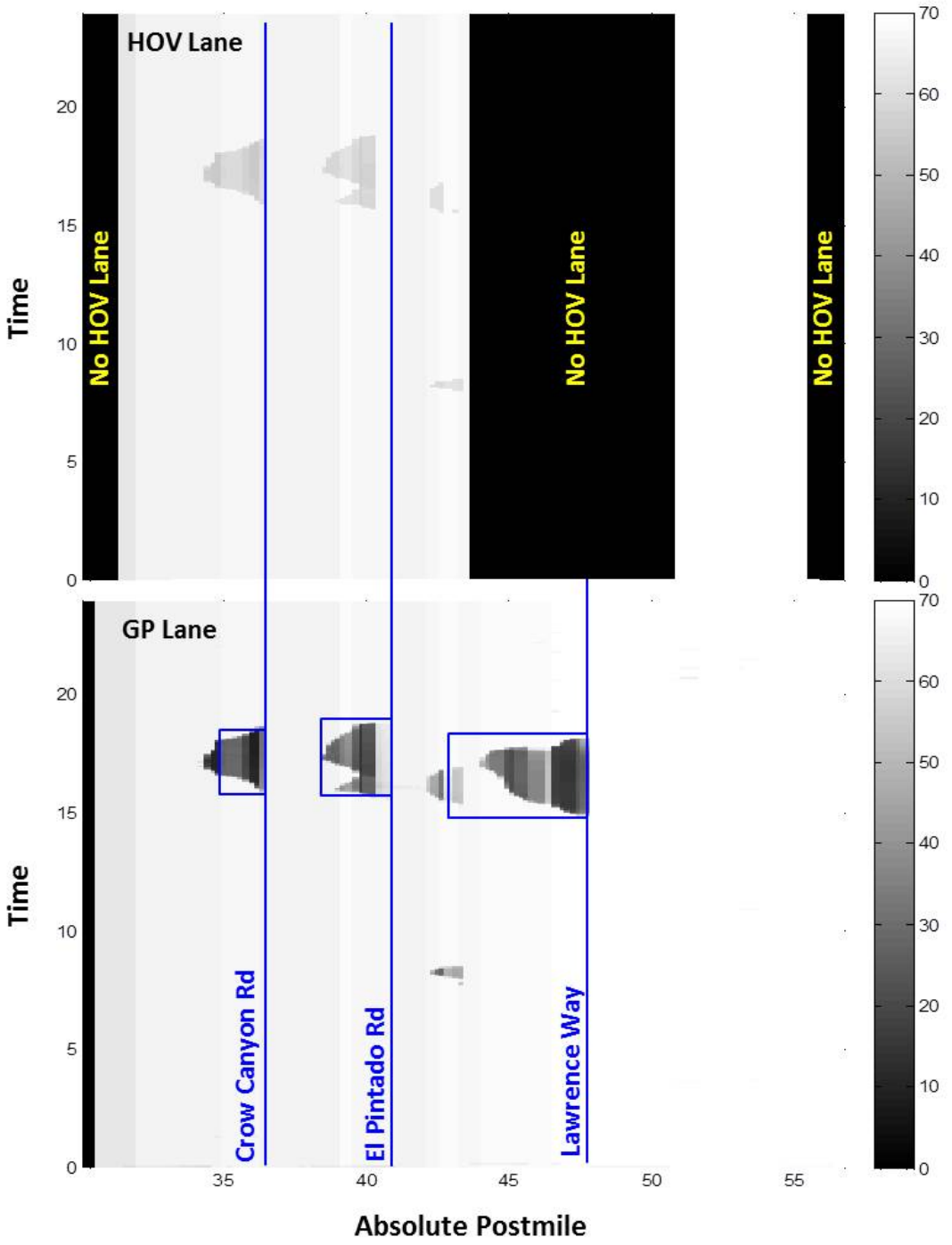

Figure 3.2: I-680 North speed contours for GP and HOV lanes produced by simulation. Speed values are given in miles per hour. Blue boxes on the GP lane speed contour indicate congested areas as identified by the I-680 CSMP study.

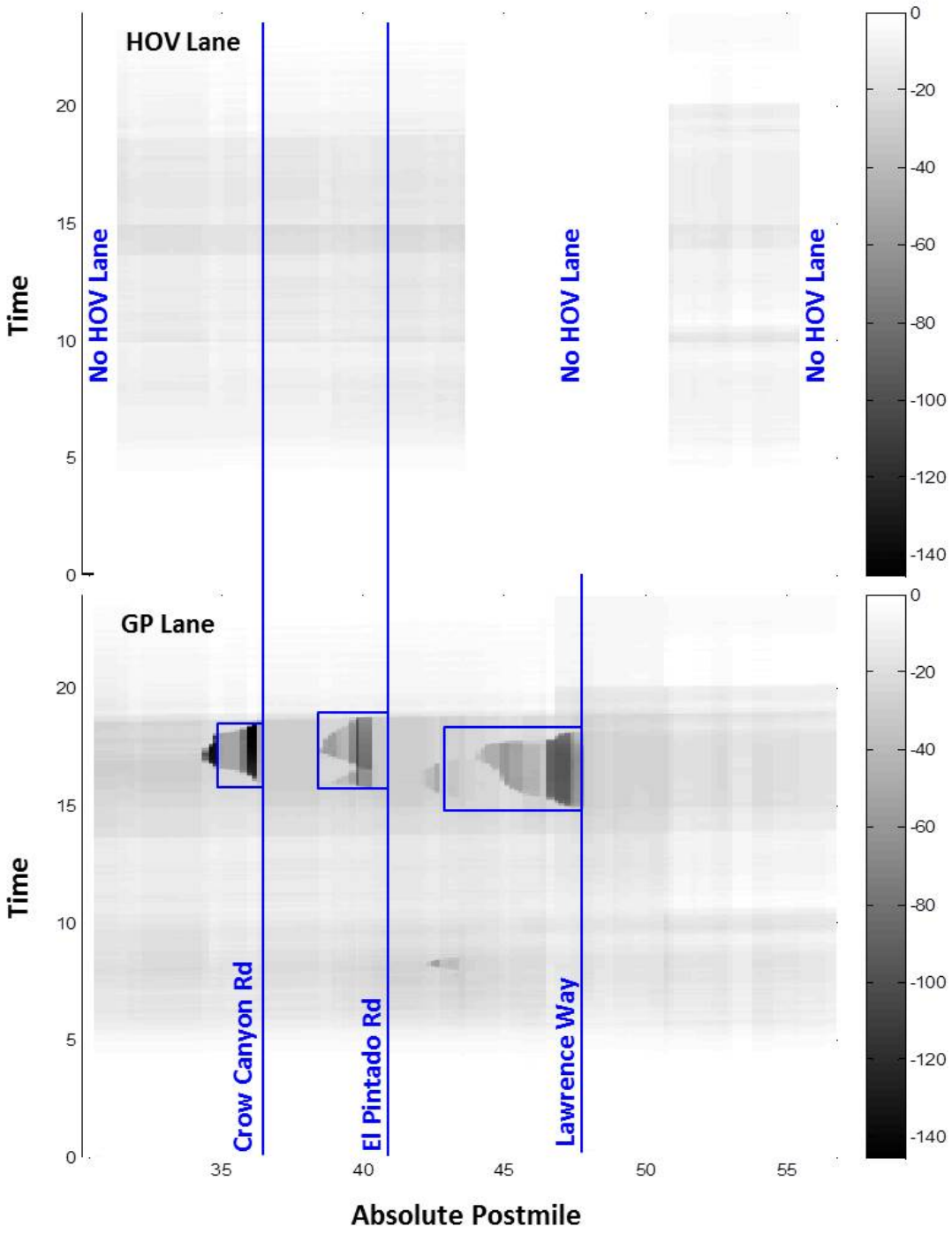

Figure 3.3: I-680 North density contours for GP and HOV lanes produced by simulation. Density values are given in vehicles per mile per lane. Blue boxes on the GP lane speed contour indicate congested areas as identified by the I-680 CSMP study.

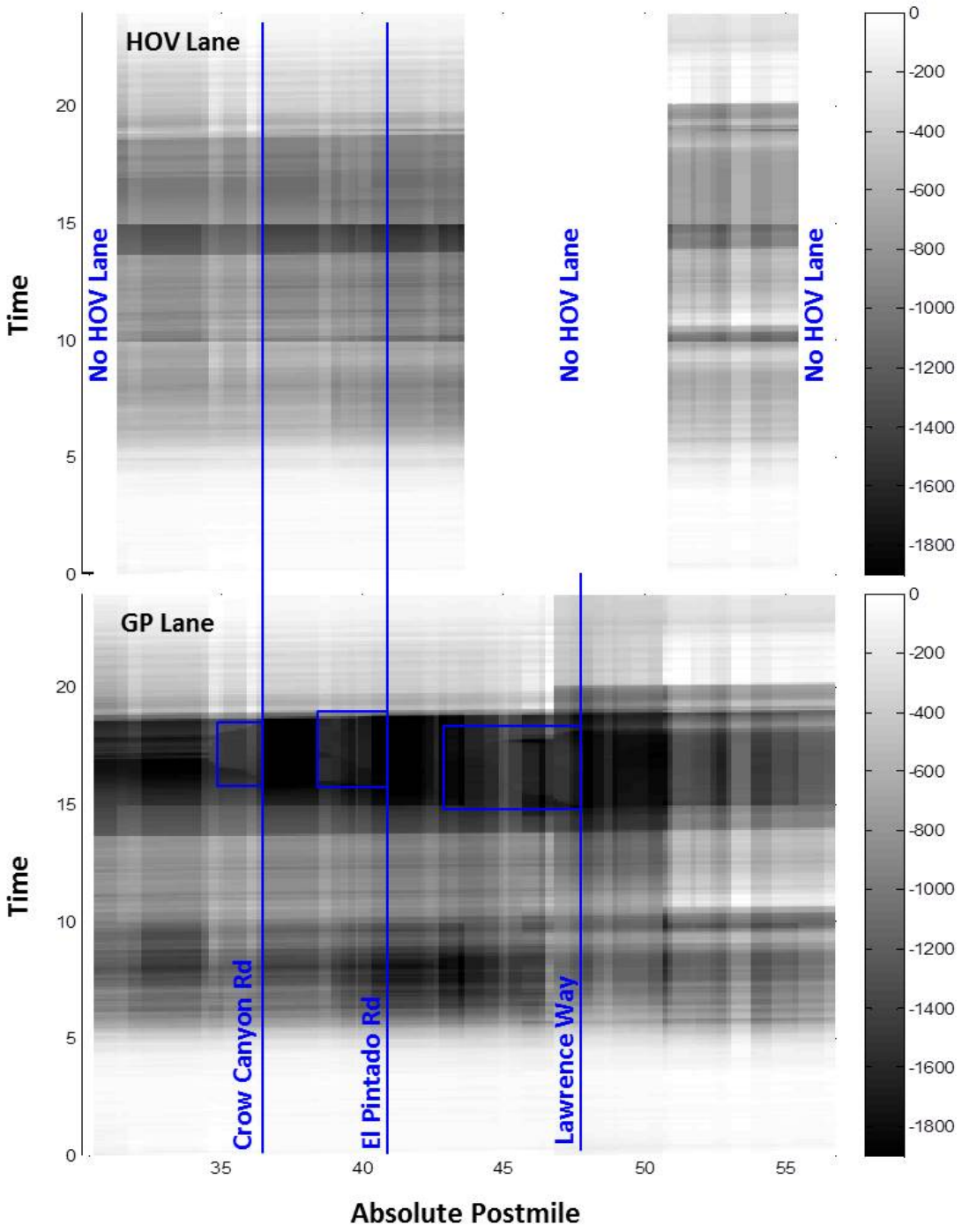

Figure 3.4: I-680 North flow contours for GP and HOV lanes produced by simulation. Flow values are give in vehicles per hour per lane. Blue boxes on the GP lane speed contour indicate congested areas as identified by the I-680 CSMP study.

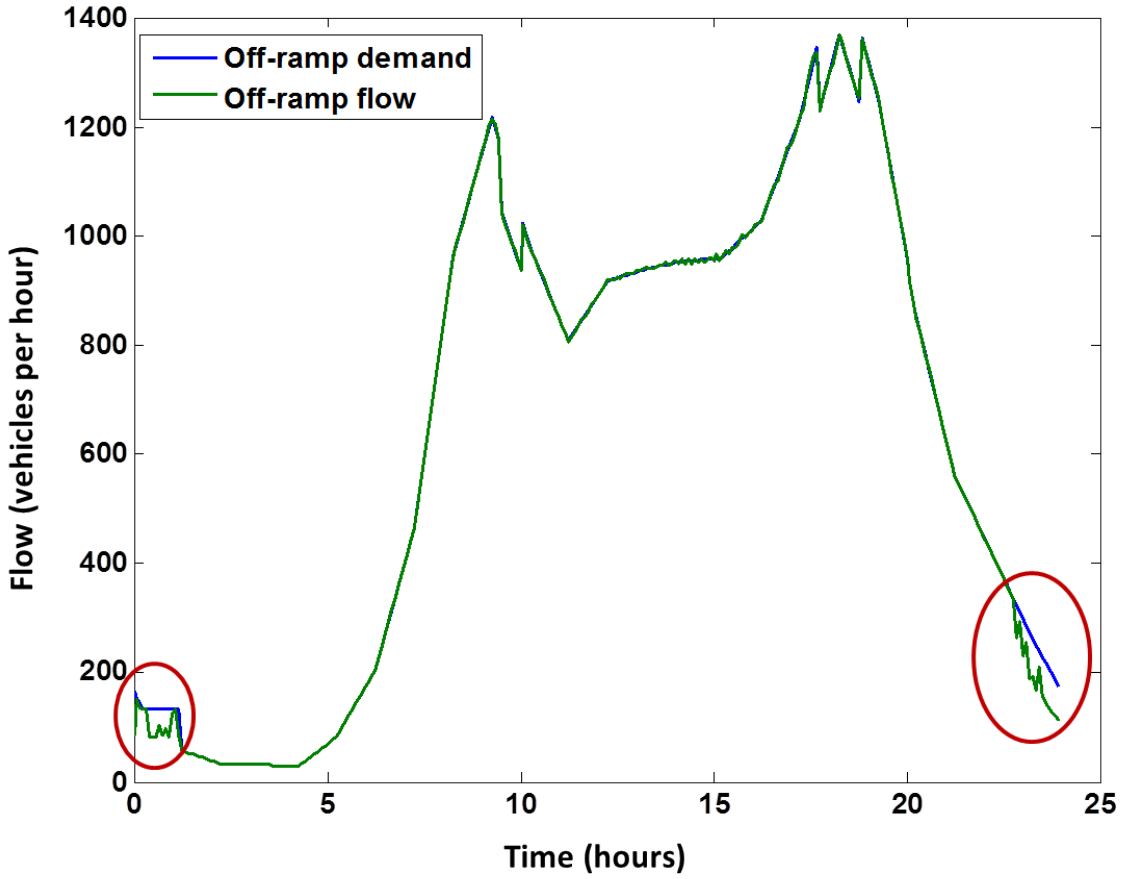

Figure 3.5: Flow at the Crow Canyon Road off-ramp over 24 hours — collected (off-ramp demand) vs. computed by simulation (off-ramp flow).

Chapter 4

Control Access HOV Lane: I-210 East

We consider a 20.6-mile stretch of SR-134 East/ I-210 East in Los Angeles County shown in Figure 4.1, as a test case for the separated HOV lane configuration. This freeway stretch consists of 3.9 miles of SR-134 East from postmile 9.46 to postmile 13.36 and 16.7 miles of I-210 East from postmile 25 to postmile 41.7. Gate locations, where traffic can switch between the GP and the HOV lanes are marked on the map. The HOV lane is always active. There are 28 on-ramps and 25 off-ramps. The largest number of off-ramps between two gates is 5. Thus, our freeway model has 7 vehicle classes - LOV, HOV and 5 destination-based.

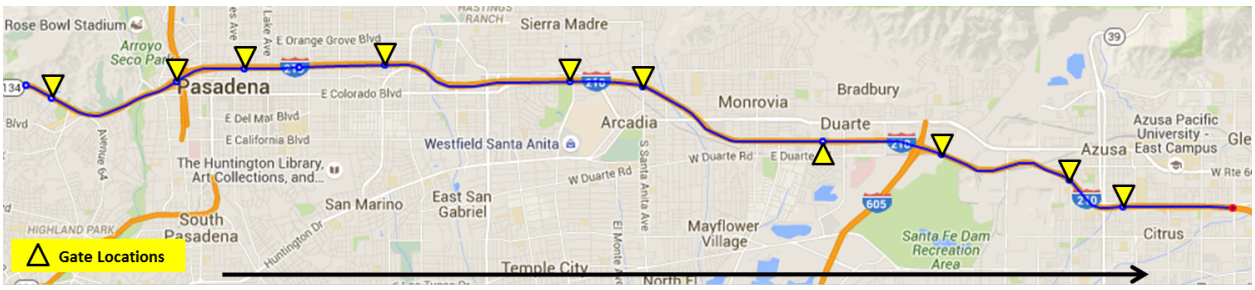

Figure 4.1: Map of SR-134 East/ I-210 East freeway in Los Angeles County.

To build the model, we used PeMS data for the corresponding segments of the SR-134 East and I-210 East for Monday, October 13, 2014 [3]. This was one of the days when most vehicle detectors on the GP and the HOV lanes, on-ramps and off-ramps of SR-134 East and I-210 East were intact, and hence the PeMS data are reliable. Fundamental diagrams were calibrated using PeMS data

following the methodology [6]. As in the I680 North example, we assume that HOV portion of the input demand is 15%.

The modeling results are presented in Figures 4.2, 4.3 and 4.4 showing speed, density and flow contours in the GP and the HOV lanes respectively. Each of these plots consists of the top, corresponding to the HOV lane, and bottom, corresponding to the GP lane, parts. As before, in all the plots traffic moves from left to right along the "Absolute Postmile" axis, while the vertical axis represents time. HOV lane does not get congested. Dashed blue lines on the contour plots indicate HOV gate locations.

Figure 4.5 shows the PeMS speed contours for the SR-134 East/ I-210 East GP and HOV lanes hat were used as a target for our simulation model. In these plots, traffic also travels from left to right, with the horizontal axis representing postmiles, while the vertical axis represents time. Note that each of the four speed contours has its own color scale (feature of PeMS).

Figure 4.6 shows an example of how well the off-ramp flow computed by the simulation matches the target, referred to as *off-ramp demand*, taken from the off-ramp at North Hill Avenue. The simulated off-ramp flow matches the off-ramp demand not perfectly, but closely enough. So is the case for all the other off-ramps.

Finally, Table 4.1 summarizes the performance measurements — VMT, VHT and delay — computed by simulation versus obtained from PeMS. PeMS data come from both SR-134 East and I-210 East, and VMT, VHT and delay values are computed as sums of the corresponding values from these two freeway sections. Delay values are computed in vehicle-hours for those vehicles travelling slower than 45 mph.

	Simulation result	PeMS data
GP Lane VMT	2,017,322	-
HOV Lane VMT	378,485	-
Total VMT	2,395,807	414,941 + 2,006,457 = 2,421,398
GP Lane VHT	33,533	-
HOV Lane VHT	6,064	-
Total VHT	39,597	6,416 + 36,773 = 43,189
GP Lane Delay	3,078	-
HOV Lane Delay	584	-
Total Delay	3,662	1 + 3,802 = 3,803

Table 4.1: Performance measures for SR-134 East/ I-210 East.

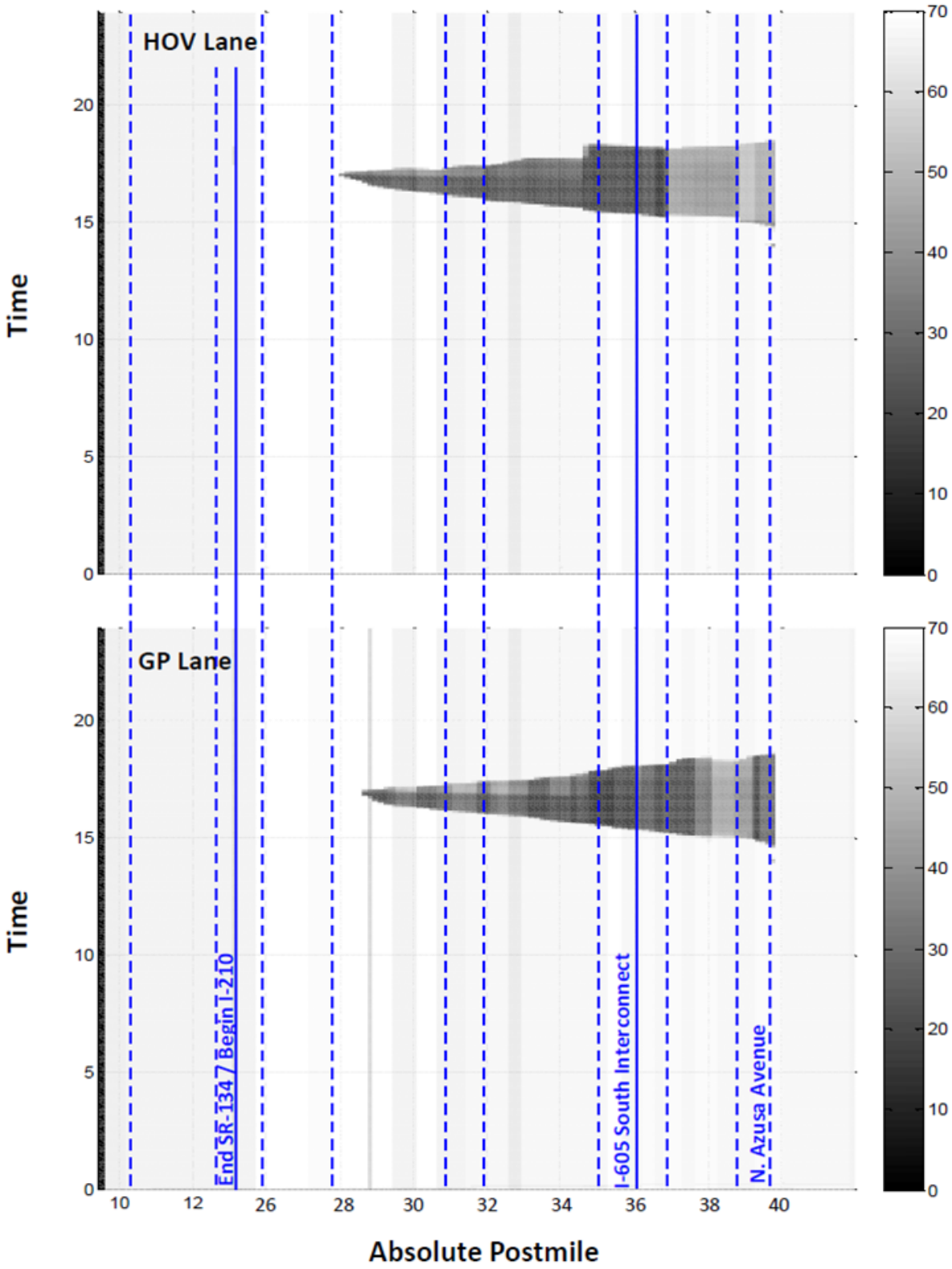

Figure 4.2: SR-134 East/ I-210 East speed contours for GP and HOV lanes produced by simulation. Speed values are given in miles per hour.

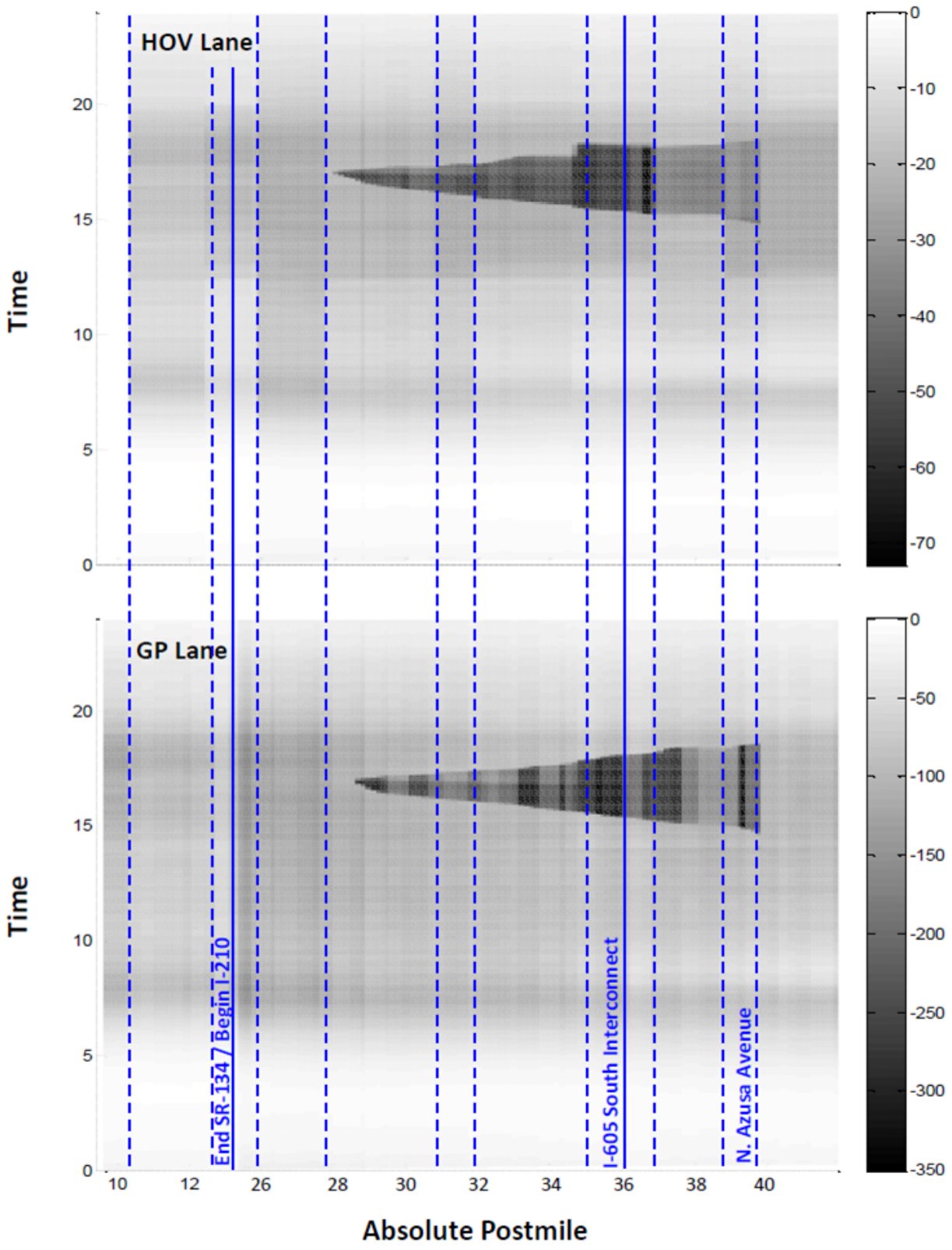

Figure 4.3: SR-134 East/ I-210 East density contours for GP and HOV lanes produced by simulation. Density values are given in vehicles per mile per lane.

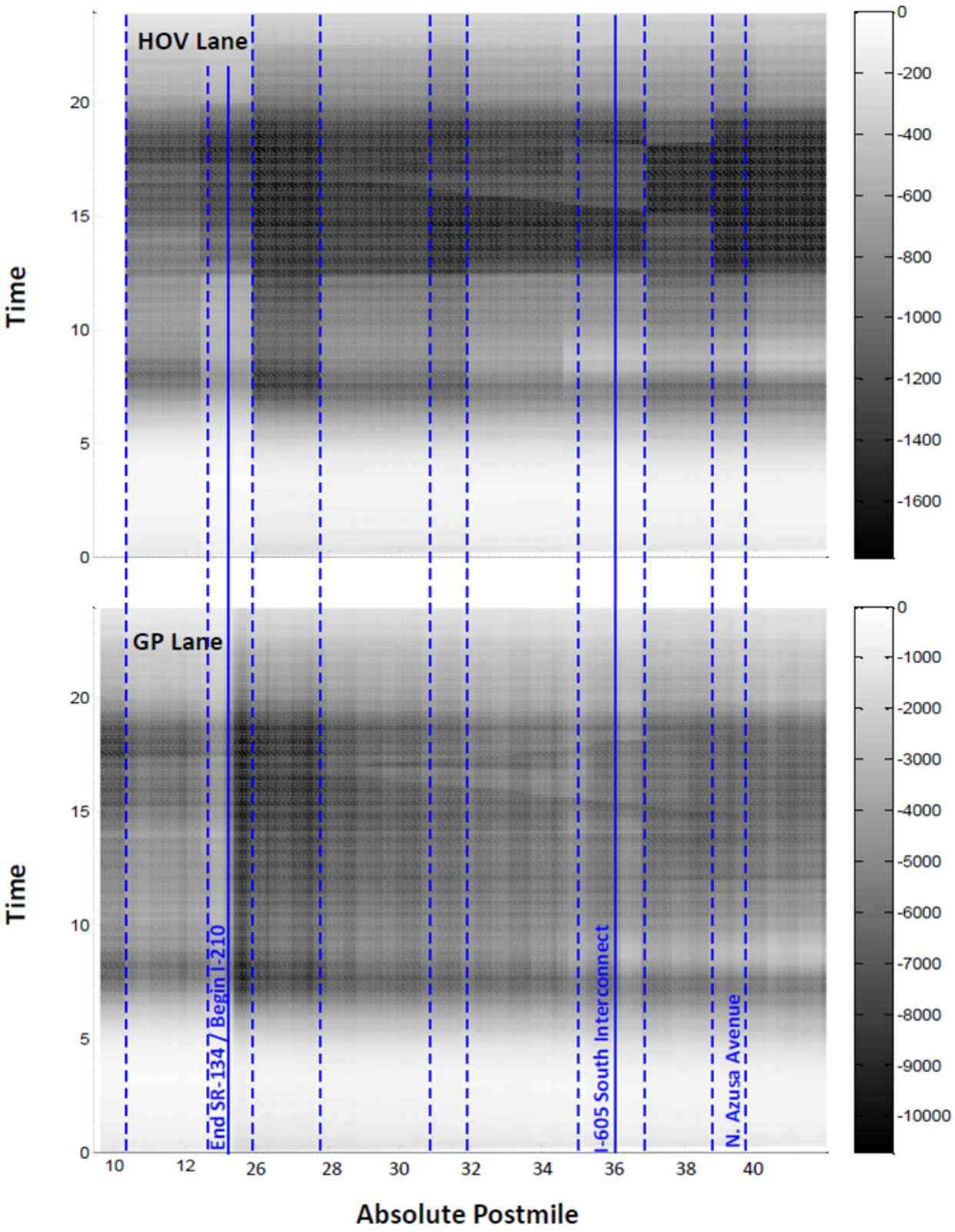

Figure 4.4: SR-134 East/ I-210 East flow contours for GP and HOV lanes produced by simulation. Flow values are give in vehicles per hour per lane.

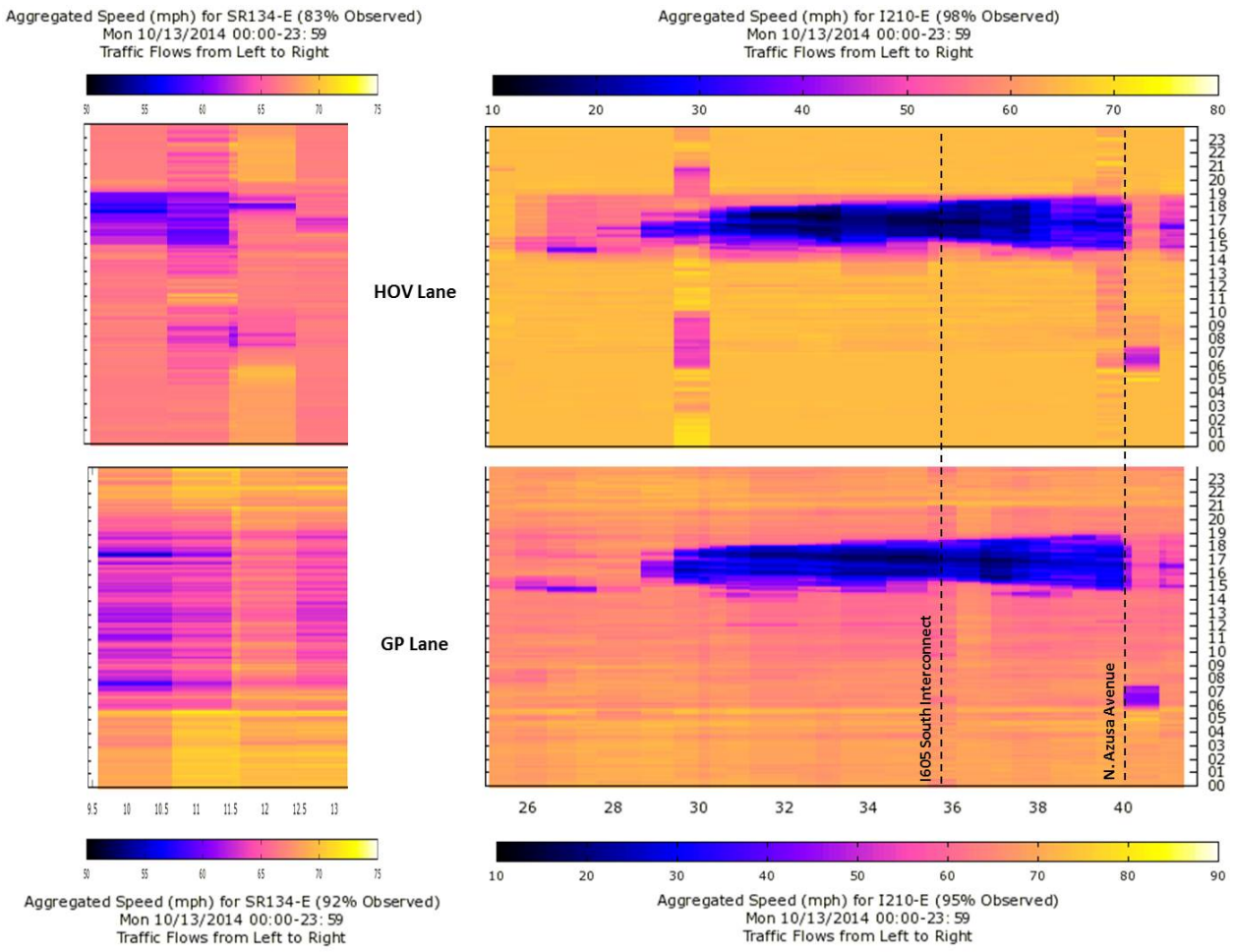

Figure 4.5: SR-134 East/ I-210 East speed contours for GP and HOV lanes obtained from PeMS [3] for Monday, October 13, 2014. Horizontal axis represents Absolute postmile, and vertical axis represents time in hours.

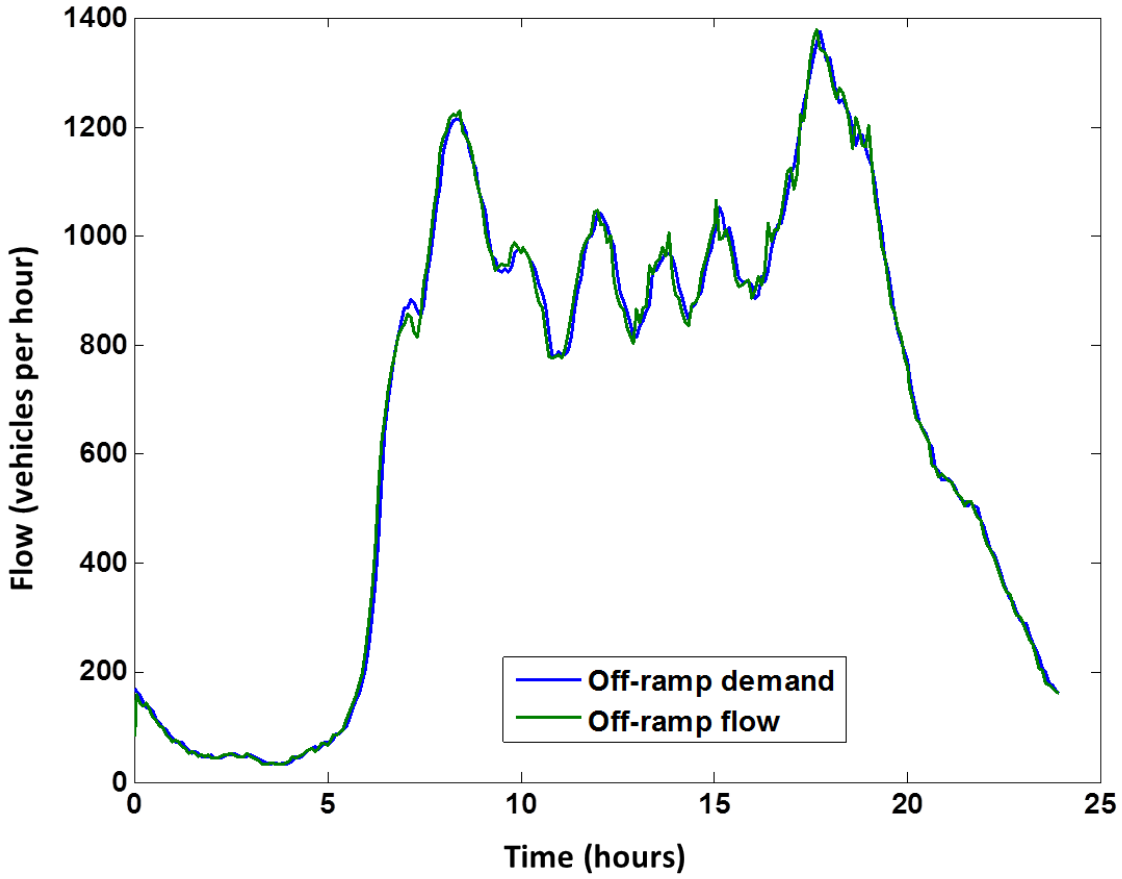

Figure 4.6: Flow at the North Hill Avenue off-ramp over 24 hours — PeMS data (off-ramp demand) vs. computed by simulation (off-ramp flow).

Chapter 5

HOT Lane: I-10 West

To evaluate the proposed model of the HOT controller, we use data from the HOT lane on I-10 West freeway in Los Angeles County [12], a 14-mile freeway with 2 ingress-only, 2 egress-only and 2 ingress/egress gates.[1] In our example we focus on one ingress/egress gate located immediately upstream of South Fremont Avenue exit, shown in Figure 5.1.

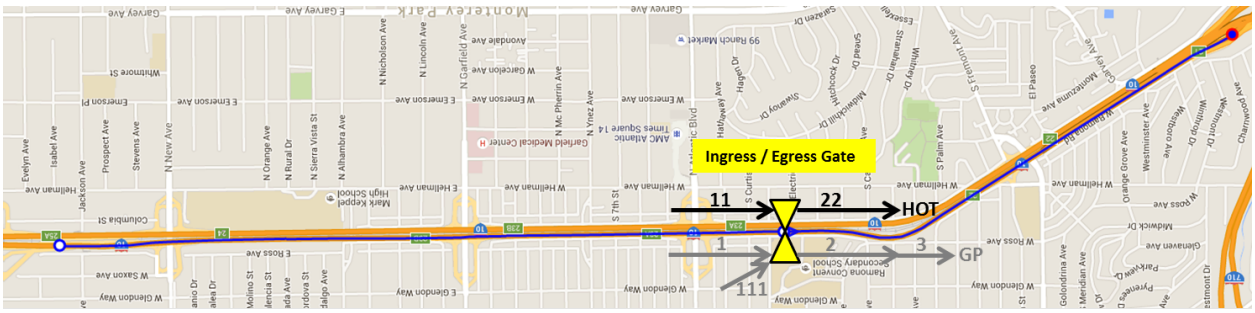

Figure 5.1: Map of the I-10 West freeway section in Los Angeles County near the studied ingress/egress HOT gate.

Here, the GP lane has 4 and the HOT lane has 2 sublanes. The HOT lane is always active, but it has two regimes corresponding to peak hours — from 5 to 9 am and from 4 to 7 pm on weekdays; and to off-peak hours — the rest of the time. During off-peak hours HOVs with two passengers or

[1]Ingress-only gate allows vehicles only to enter the HOT lane. Typically, ingess-only gates are at on-ramps that are directly connected to the HOT lane. Egress-only gate allows vehicles only to exit the HOT lane. Typically, egress-only gates are at off-ramps, to which the HOT lane is connected directly. Ingress/egress gate is a stretch of freeway, where traffic can switch between the GP and HOT lane. In the I-210 East example we dealt with ingress/egress gates.

more can use the HOT lane free of charge, and single-occupancy vehicles (SOVs) can use the HOT lane at the fixed price of 25 cents per mile. During peak hours HOVs with three passengers or more can use the HOT lane free of charge. The others are considered LOVs and to use the HOT lane have to pay the toll that varies between 35 and 140 cents per mile depending on the demand for the HOT lane. **Our focus is on the HOT controller behavior during peak hours when the HOT lane is dynamically priced between 35 and 140 cents per mile.**

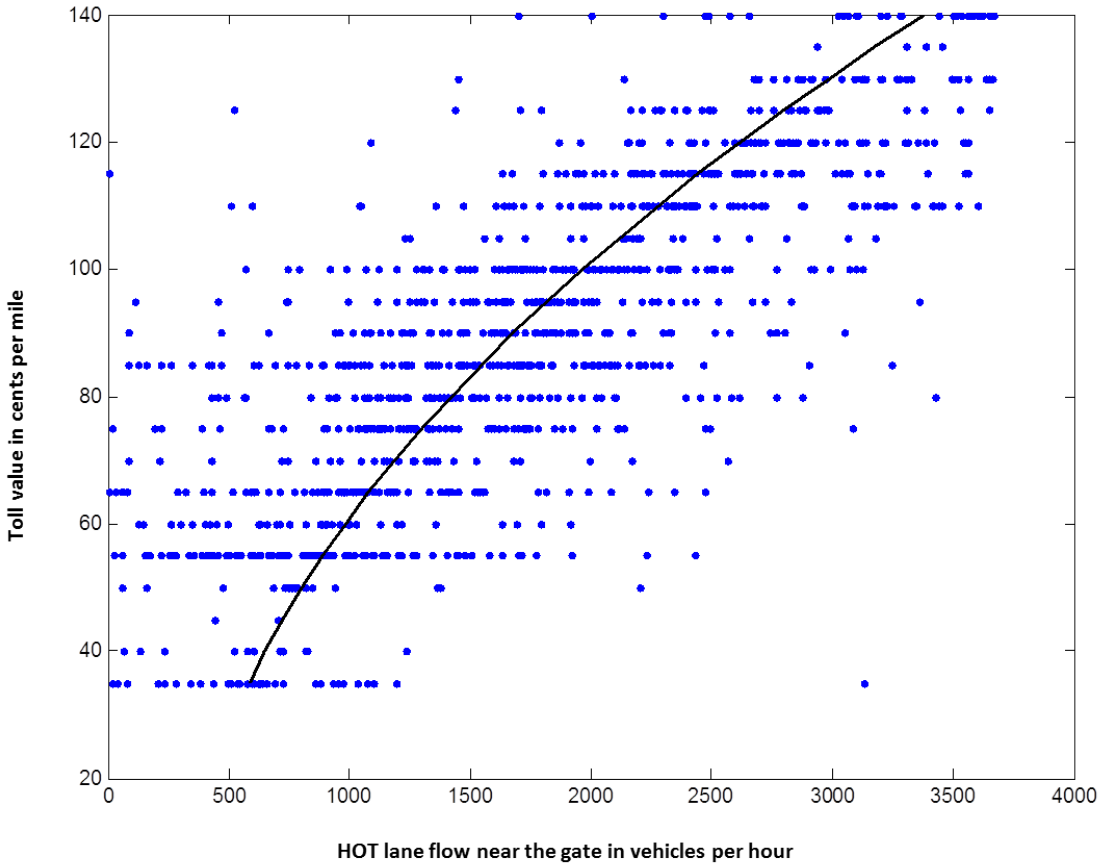

Figure 5.2: Estimation of the toll value based on the flow in the HOT lane.

We used I-10 West toll data for the year 2014 obtained from LA Metro [12] to calibrate and test the HOT controller. These vehicle counts are collected through FasTrak readers that label each vehicle based on its transponder setting as HOV-3 (3 passengers or more), HOV-2 (2 passengers or more) or SOV. Thus, we know not only the vehicle flow near the FasTrak reader, but how this flow breaks down into HOV and LOV portions.

Remark. Sometimes drivers cheat: a certain number of vehicles with the FasTrak transponder set to HOV-3 are, in fact, SOVs. Our model **does not** identify cheaters. It should be used for assessment of freeway operation provided that there is a given number of self-declared SOVs, HOV-2s and HOV-3s.

We start by building the dependency of the toll value on the vehicle flow in the HOT lane. Figure 5.2 shows this dependency. As we can see, HOT flow varies between 0 and 3,750 vehicles per hour, while the toll value changes in 5-cent increments between 35 and 140 cents per mile. Polynomial curve fitting to the data results in the toll lookup table — Table 5.1. Recall from Section 2.3 that the toll lookup table is the first part of the HOT controller model. as was mentioned there, this lookup table is typically put together by the operator of the HOT facility. For the purpose of this example, however, we estimated it from the I-10 West toll data.

HOT lane flow in vehicles per hour	Toll value in cents per mile
585	35
651	40
724	45
804	50
890	55
983	60
1,082	65
1,188	70
1,301	75
1,421	80
1,547	85
1,680	90
1,820	95
1,966	100
2,119	105
2,279	110
2,446	115
2,619	120
2,799	125
2,985	130
3,178	135
3,378	140

Table 5.1: Toll lookup table.

The second part of the HOT controller, according to Section 2.3, is the calculation of the portion of LOV traffic ready to pay for using the HOT lane. We obtain the measurement of readiness to

pay $\hat{\rho}^t$ from relation (2.4.1) using the I-10 West toll data that allow us to extract the LOV portion of the vehicle counts in the HOT lane for the nominator, and PeMS data for the Vehicle Detector Station (VDS) 716101 [3] for the denominator of the right-hand side of (2.4.1). [2]

Figure 5.3 shows the dependency of $\hat{\rho}^t$ on the difference of vehicle densities in the GP and the HOT lanes obtained from the PeMS VDS 716101 (left), and on the toll value (right). We estimate the portion of LOV traffic ready to pay, ρ, according to the expression (2.3.2), as a function of both the GP-HOT density difference and the toll value. Since we have 4 GP and 2 HOT lanes, following (2.4.3),

$$\alpha_0 = \ln(2/4) = -0.6931.$$

From the least squares fit (2.4.5)-(2.4.6), we get

$$\alpha_1 = 0.0115, \quad \alpha_2 = -0.0053.$$

Figure 5.4 shows the surface fitting to the data. The resulting readiness to pay ρ as a function of GP-HOT density difference and toll is shown as a 2-dimensional contour in Figure 5.5.

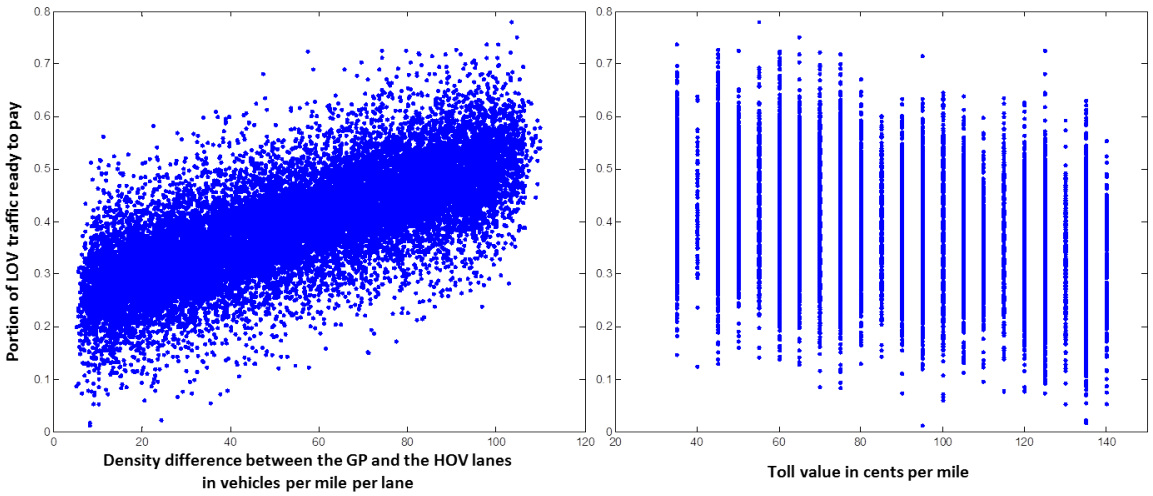

Figure 5.3: Dependency of rediness to pay on difference of traffic density in the GP and the HOV lanes (left); and on the toll value (right).

[2] We used data for weekdays of October 2014.

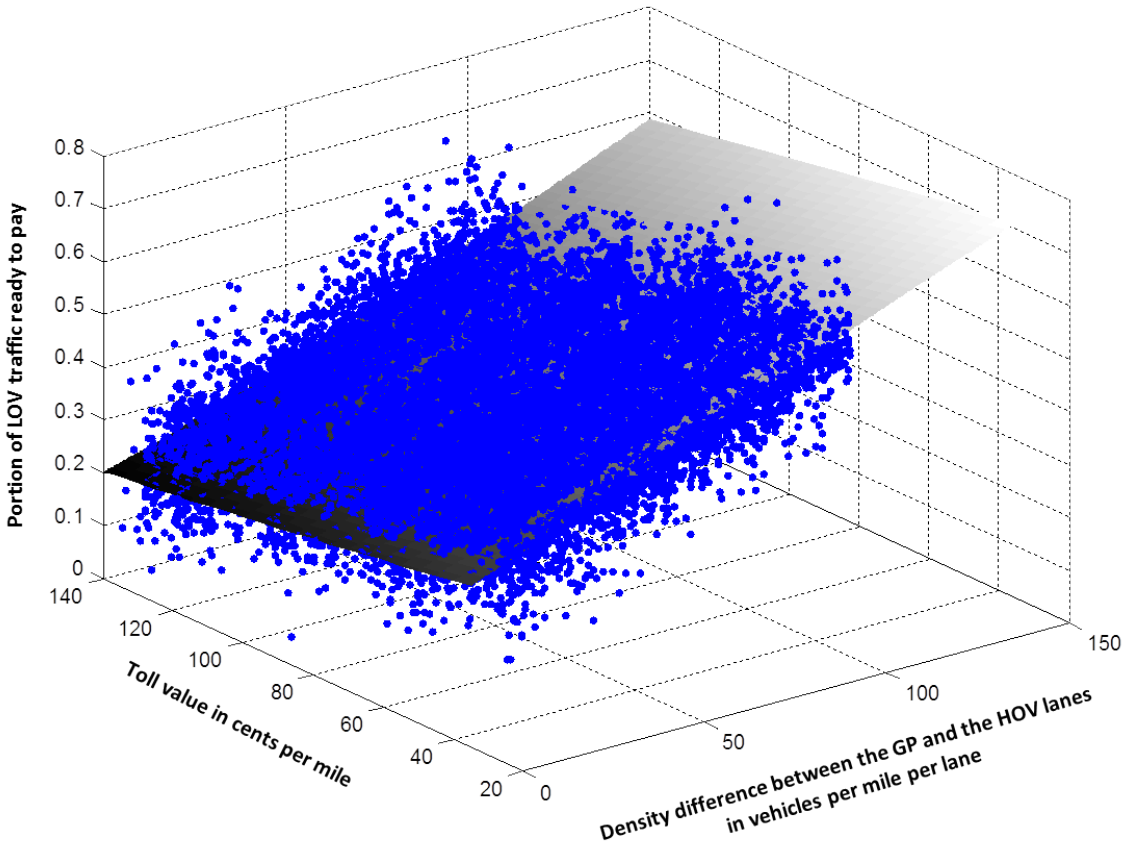

Figure 5.4: Estimation of readiness to pay as a function of density difference between the GP and the HOV lanes and the toll.

Now that the HOT controller is calibrated, we test it in three scenarios.

Scenario 1. Consider the road network configuration as shown in Figure 5.1, where link capacities are:

$$F_1 = 8,000 \text{ vph}, \quad F_2 = 8,000 \text{ vph}, \quad F_3 = 1,600 \text{ vph};$$

$$F_{11} = 3,600 \text{ vph}, \quad F_{22} = 3,600 \text{ vph};$$

$$F_{111} = 2,000 \text{ vph}.$$

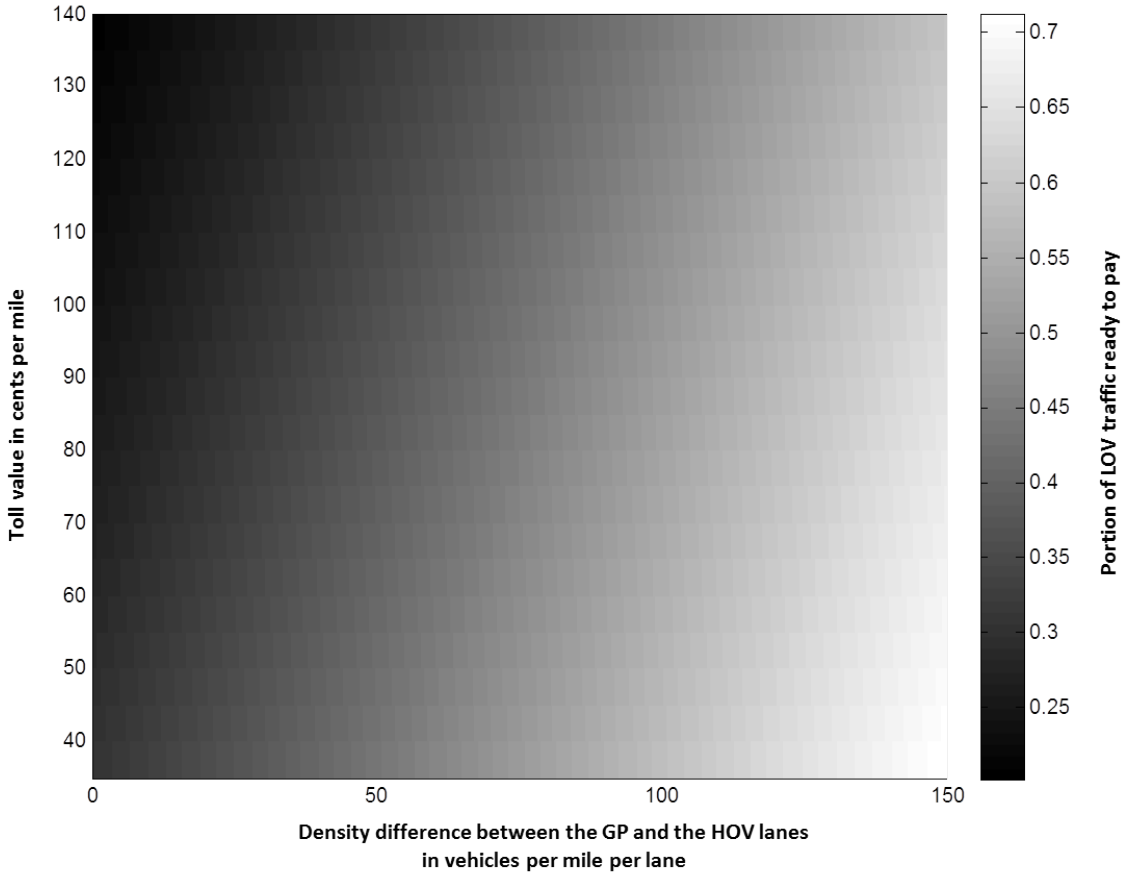

Figure 5.5: Readiness to pay as a function of density difference between the GP and the HOV lanes and the toll.

Input demand for links 1 and 11 is constant:

$$
\begin{aligned}
&d_1^1 = 6,700 \text{ vph}, \quad d_1^2 = 0 \text{ vph}, \quad d_1^3 = 0 \text{ vph};\\
&d_{11}^1 = 0 \text{ vph}, \quad d_{11}^2 = 385 \text{ vph}, \quad d_{11}^3 = 0;\\
&d_{111}^1 = 85 \text{ vph}, \quad d_{111}^2 = 15 \text{ vph}, \quad d_{111}^3 = 0 \text{ vph}.
\end{aligned}
$$

As we can see, GP link 3 with its low capacity creates a bottleneck for traffic that stays in the GP lane.

Figure 5.6 presents the results of the simulation: LOV and HOV input demand (top-left); flows entering the GP link 2 and the HOT link 22 (bottom-left); toll value (top-right); and the portion of LOV traffic ready to pay the corresponding toll. The system reaches the equilibrium at 80 cents

per mile with 37% of LOVs ready to pay.

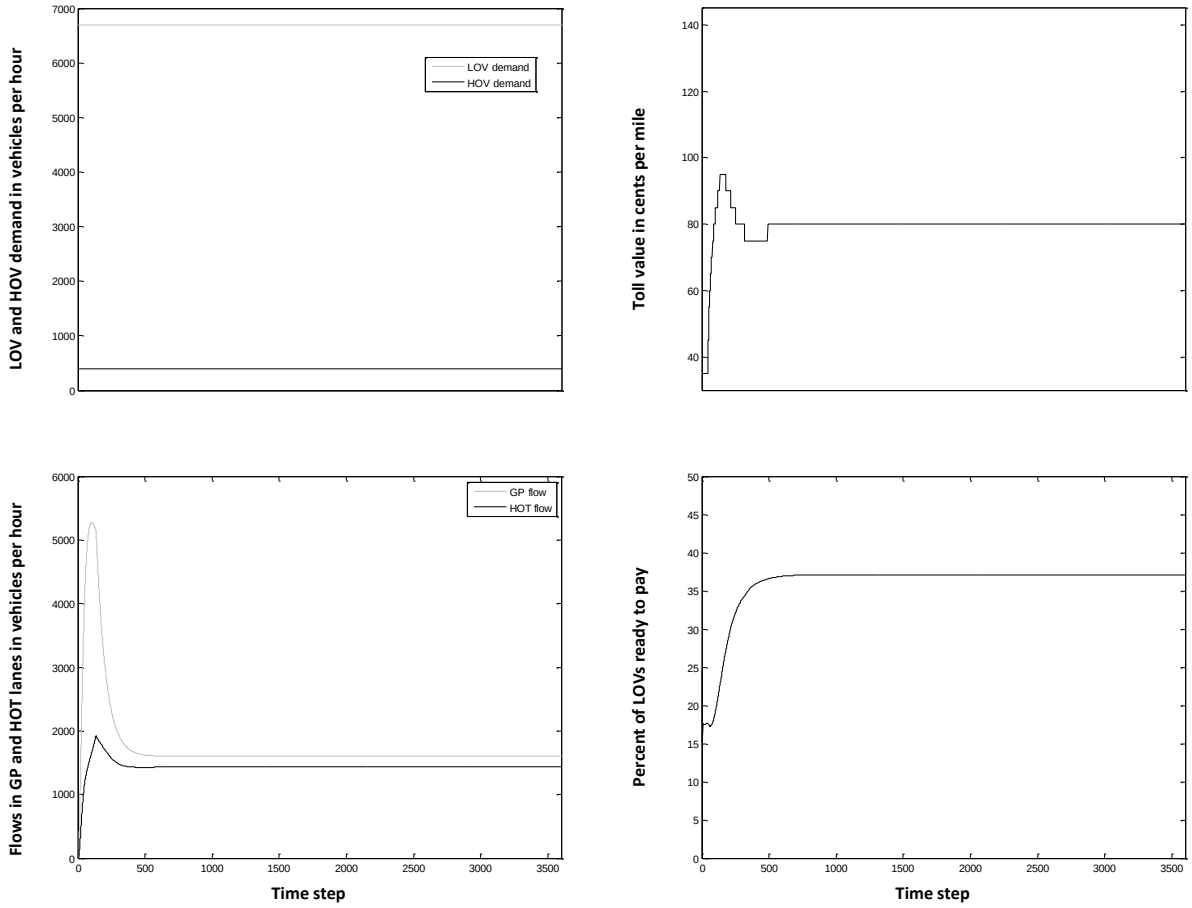

Figure 5.6: Scenario 1 — constant LOV and HOV demand.

Scenario 2. This scenario differs from the scenario 1 only in the HOV demand coming into the HOT lane:

$$d_{11}^2 = 2,585 \text{ vph.}$$

As shown in Figure 5.7, more vehicles enter now the HOT link 22 (bottom-left); the toll value goes up accordingly, to 135 cents per mile; and the readiness to pay drops to 27%.

Scenario 3. In this scenario, we set capacity of the GP link 3:

$$F_3 = 7,600 \text{ vph.}$$

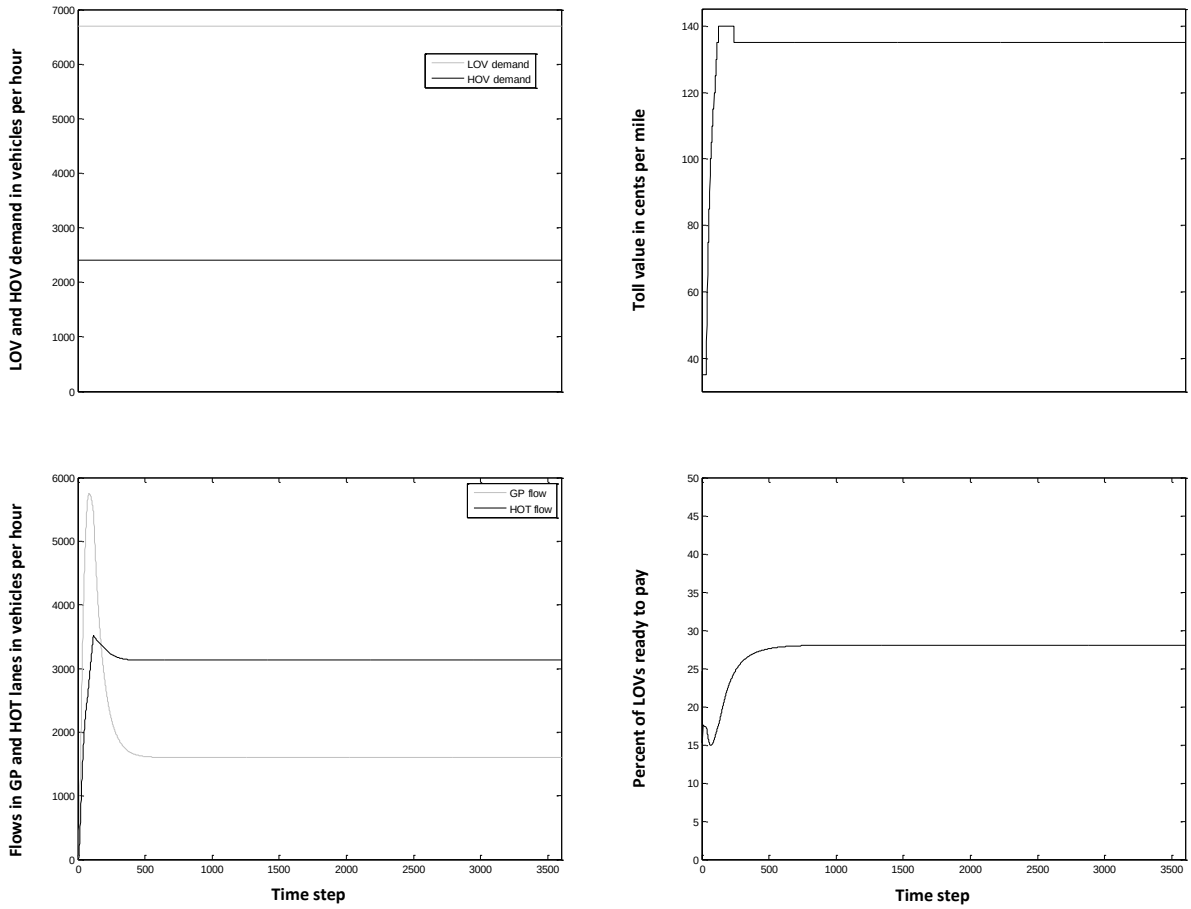

Figure 5.7: Scenario 2 — the same as scenario 1, but has higher HOV demand.

The simulation is divided into 4 time periods. The LOV and the HOV demand in links 1 and 11 changes from period to period as specified in Table 5.2.

	Time period 1	Time period 2	Time period 3	Time period 4
d_1^1 (vph)	7,000	7,600	4,000	6,000
d_{11}^2 (vph)	2,940	940	1,940	2,440

Table 5.2: Varying demand.

On-ramp demand is constant:

$$d_{111}^1 = 340 \text{ vph}, \quad d_{111}^2 = 60 \text{ vph}.$$

The results of the simulation are shown in Figure 5.8.

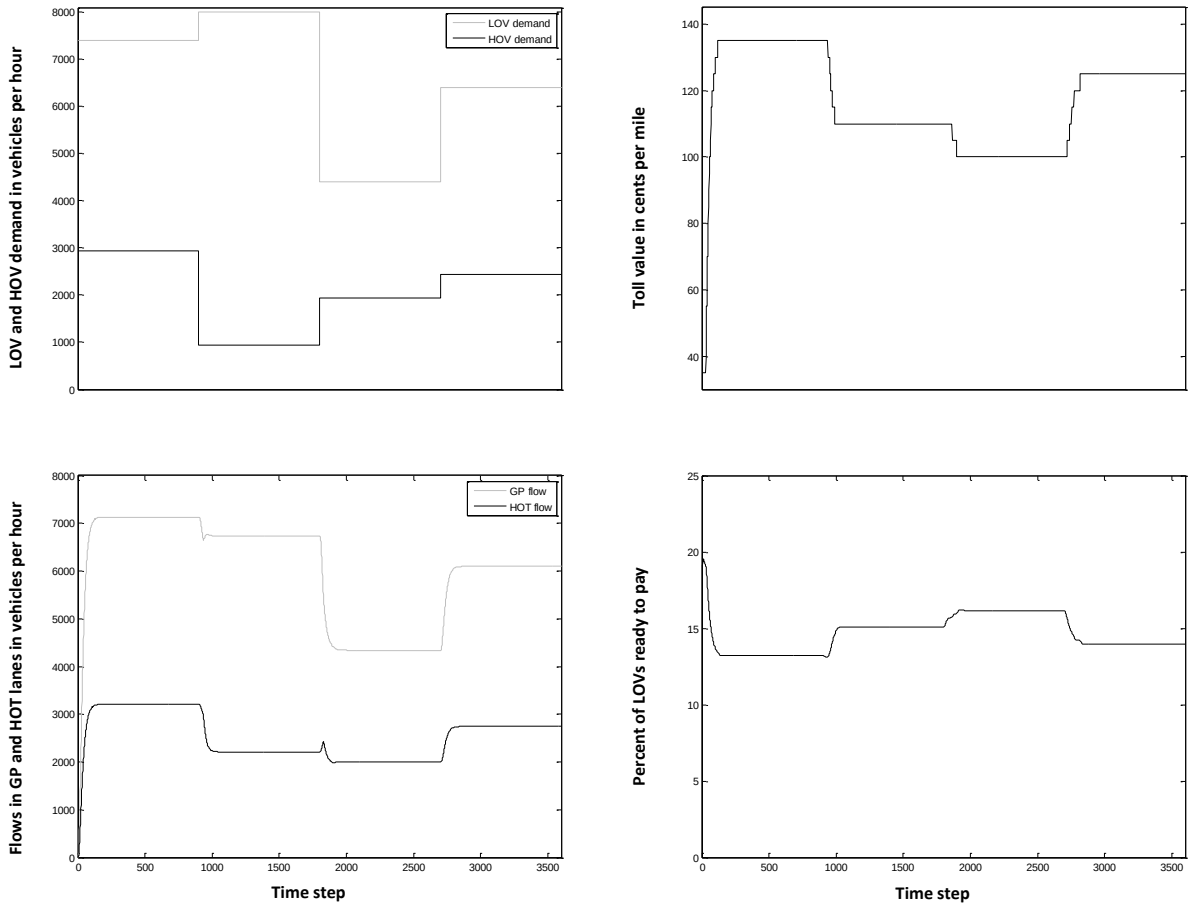

Figure 5.8: Scenario 3 — varying LOV and HOV demand.

As was mentioned above, we treat the FasTrak transponder data as ground truth when tuning the HOT controller. The model does not account for cheating behavior on the part of the SOV drivers who declare themselves as HOVs. Yet, such behavior exists: Table 5.3 shows the comparison of vehicle counts breakdown by vehicle category, SOV, HOV-2 and HOV-3, between FasTrak readings and manual counts. Evidently, a large number of HOV-3s are actually SOVs. Further research is needed for developing the model of cheating behavior.

Vehicle category	FasTrak counts and breakdown	Manual counts and breakdown
SOV	1567 (52.5%)	2069 (82.6%)
HOV-2	338 (11.3%)	334 (13.3%)
HOV-3	1082 (36.2%)	101 (4%)
Total	2987	2504

Table 5.3: Vehicle counts collected on September 26, 2013 (Thursday), during AM peak hours, between 7 and 8 am, on the segment of I-10 West shown in Figure 5.1. Source: Caltrans District 7.

Chapter 6

Conclusion

In the course of this project a macroscopic simulation model for freeways with managed lanes was developed. It was implemented in the Berkeley Advanced Traffic Simulator (BeATS) [1] and tested for I-680 North, I-210 East freeways, as well as toll control using FasTrak transponder data from I-10 West. As test examples show, the model can adquately represent traffic behavior in the presence of multiple vehicle classes and managed lane facilities. Model calibration methodology is provided.

This project is a step in the development of the open source software toolbox for evaluation of transportation planning and operational scenarios. Building on the results of the current project, such toolbox can be extended to include the following capabilities:

- Given a traffic pattern, estimate HOT revenue projections;
- Optimize dynamic toll strategy;
- Optimize ramp metering plans;
- Determine the cause of congestion — excessive demand or poor operational strategy;
- Specify demand in a destination-based fashion and obtain more accurate future year projections based on the input from the 4-step demand model;
- Include arterial signals adjacent to freeway on- and off-ramps.

In Chapter 5 we emphasized that the proposed HOT controller has no knowledge about cheaters, SOVs that declare themselves HOVs to avoid the toll, and uses data collected from FasTrak transponders as is. Caltrans District 7 expressed interest in analyzing the impact of cheating behavior on the freeway operation and the collected revenue.

As the next research step, we recommend extending the present HOT model to incorporate data such as given in Table 5.3 and to add the new vehicle class *cheater*. Such model extension would enable the analysis of operational and revenue impacts of the cheating behavior.

Bibliography

[1] Berkeley Advanced Traffic Simulator. `http://github.com/calpath/beats`.

[2] Connected Corridors Program. `http://connected-corridors.berkeley.edu`.

[3] California Department of Tranportation. PeMS homepage. `http://pems.dot.ca.gov`.

[4] Michael J. Cassidy, Kwangho Kim, Wei Ni, and Weihua Gu. A problem of limited-access special lanes. Part I: Spatiotemporal studies of real freeway traffic. *Transportation Research Part A: Policy and Practice*, In press, 2015.

[5] R. Courant, K. Friedrichs, and H. Lewy. Über die partiellen Differenzengleichungen der mathematischen Physik. *Mathematische Annalen*, 100(1):32–74, 1928.

[6] G. Dervisoglu, G. Gomes, J. Kwon, A. Muralidharan, P. Varaiya, and R. Horowitz. Automatic calibration of the fundamental diagram and empirical obsevations on capacity. *88th Annual Meeting of the Transportation Research Board, Washington, D.C., USA*, 2009.

[7] K. Jang and M. Cassidy. Dual influences on vehicle speed in special-use lanes and critique of US regulation. *Transportation Research, Part A*, 46(2012):1108–1123, 2012.

[8] Kitae Jang, Sanghyouk Oum, and Ching-Yao Chan. Traffic Characteristics of High-Occupancy Vehicle Facilities. *Transportation Research Record: Journal of the Transportation Research Board*, 2278:180–193, 2012.

[9] A. A. Kurzhanskiy and P. Varaiya. Active traffic management on road networks: a macroscopic approach. *Phil. Trans. R. Soc. A*, 368:4607–4626, 2010.

[10] A. A. Kurzhanskiy and P. Varaiya. Traffic management: An outlook. *Economics of Transportation*, 4(3):135–146, 2015.

[11] T. Lomax, D. Schrank, and B. Eisele. The 2012 Annual Urban Mobility Report. Technical report, Texas Transportation Institute, 2012. http://mobility.tamu.edu.

[12] Los Angeles County Metropolitan Transportation Authority. Metro Express Lanes. http://www.metroexpresslanes.net.

[13] Metropolitan Transportation Commission. Bay Area Express Lanes. http://bayareaexpresslanes.org.

[14] Inc. System Metrics Group. Contra Costa County I-680 Corridor System Management Plan Final Report. Technical report, Caltrans District 4, 2015. http://dot.ca.gov/hq/tpp/corridor-mobility/CSMPs/d4_CSMPs/D04_I680_CSMP_Final_Revised_Report_2015-05-29.pdf.

[15] C. M. J. Tampère, R. Corthout, D. Cattrysse, and L. H. Immers. A generic class of first order node models for dynamic macroscopic simulation of traffic flows. *Transportation Research, Part B*, 45(1):289–309, 2011.

[16] TOPL. TOPL homepage, 2006-2011. http://ucb-trans.org/topl/.

[17] M. Wright, G. Gomes, R. Horowitz, and A. A. Kurzhanskiy. On node and route choice models for high-dimensional road networks. 2016. http://arxiv.org/abs/1601.01054.